RELAXATION OSCILLATORS BASED ON CURRENT-CONTROLLED NEGATIVE RESISTANCE

A Thesis Submitted in

Partial Fulfilment of the Requirements

For the Degree of

MASTER OF TECHNOLOGY

by

R. Kumar

to the
Department of Electrical Engineering
INDIAN INSTITUTE OF TECHNOLOGY, KANPUR

December 1974

CERTIFICATE

This is to certify that the thesis, entitled, RELAXATION OSCILLATORS BASED ON CURRENT-CONTROLLED NEGATIVE RESISTANCE is a record of the work carried out under my supervision and that it has not been submitted elsewhere for a degree.

Kanpur
December 1974

T.R. Viswanathan
Professor
Department of Electrical Engineering
Indian Institute of Technology, Kanpur

ACKNOWLEDGEMENT

I feel it my pleasant duty to express my gratitude to my Advisor, Dr. T.R. Viswanathan, under whose supervision the work reported hereinafter was carried out. Not only was he a prime mover of the research project but also he kept himself closely associated with it at all stages of the work. During the final phase when unsuspected difficulties cropped up he sustained me by active support at the work table. His major contribution, however, is to have inspired me into an abiding interest in electronics.

Thanks are due to Mr. R. Sharma, who while working for his Ph.D., rendered willing help. Mr. A.C. Joshi readily lent instruments and equipment even during odd hours, which greatly facilitated laboratory work. Mr. H.K. Nathani undertook the typing work and I feel obliged for his pleasant cooperation.

R. Kumar

Kanpur
December 1974

CONTENTS

CHAPTER 1

INTRODUCTION

Low frequency (1 Hz - 100 Hz) relaxation oscillators find many applications. For example, the most vital part of an electronic wrist-watch or a cardiac pace-maker is a stable low-frequency oscillator. Such oscillators are also used in the firing circuits of SCRs in power electronics applications and industrial timers.

The presented work is an attempt to investigate reliable and stable low frequency oscillators for these applications. The major requirements of such an oscillators are: small size, low power consumption, frequency stability with respect to ambient temperature and power supply voltage and simplicity of circuit for higher reliability and low cost.

Oscillator circuits based on two terminal negative resistance devices are well known for their simplicity. Thus, the use of a negative resistance device is considered in detail for application as a relaxation oscillator, to meet these requirements.

A current controlled negative resistance device is preferred over a voltage controlled negative resistance device since the former requires a capacitor for oscillations whereas the latter needs an inductor.

Small size can readily be achieved by fabricating the circuit in integrated circuit form (except for the timing elements).

The present day technique of obtaining stable low frequency oscillations is to start with a stable crystal oscillator. This requires a rather complex count-down circuitry [1] [2]. The aim of the project is to design relaxation oscillators which oscillate in the range of 1MHz. This obviates the need for count-down circuits.

The stability in frequency that can be achieved by this direct method is investigated with the view to determine the limits that can be achieved. In other words, the causes of instability are examined in detail and compensation schemes are tried to reduce sensitivity of frequency with respect to variation in circuit parameters arising from changes in ambient temperature and power supply voltage.

CHAPTER 2

R ELAXATION OSCILLATOR

21 Piece-wise Linear Current-Controlled Negative Resistance

Let us assume that we have a piece-wise linear current controlled negative resistance device (CCNR) whose terminal characteristics are shown in Figure (2.1). It is well known that relaxation oscillations are readily obtained by using the NR device in the circuit configuration shown in Figure (2.2). The period of oscillations of the circuit is derived in terms of the circuit and device parameters.

2.2 Bias Condition

The supply voltage E and resistance R_L are chosen in such a way that the load line intersects the characteristics at a single point Q (Figure 2.1) on the negative resistance region of the characteristics. Since, at the point Q, the circuit is unstable, a small perturbation will cause the circuit to oscillate and the trajectory of the operating point will be as shown in Figure (2.1)i [A B C D A]. In other words, the point of operation will move along this trajectory. The time taken for one period will now be evaluated in terms of the time taken for the operating point to traverse the segments AB, BC, CD and DA.

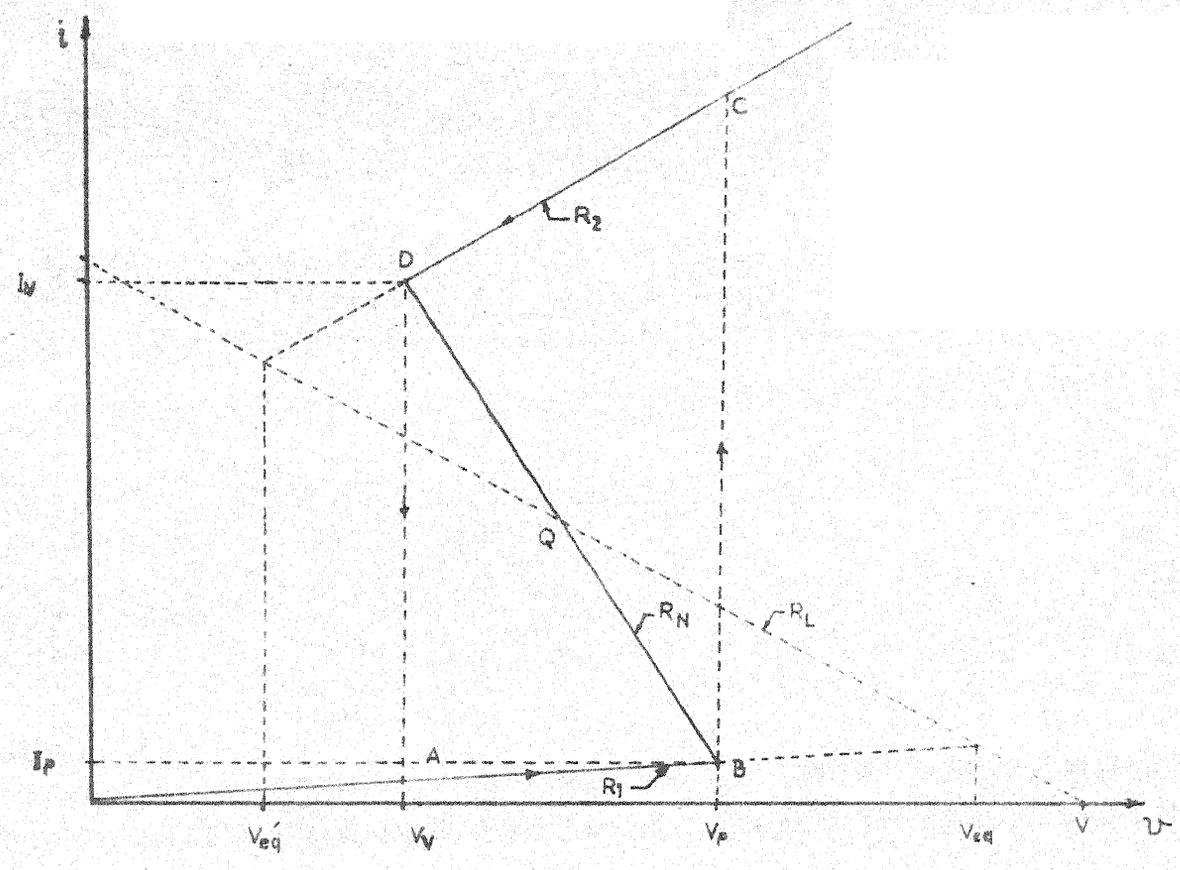

FIG. (2.1)

PIECE-WISE LINEAR CCNR CHARACTERISTICS

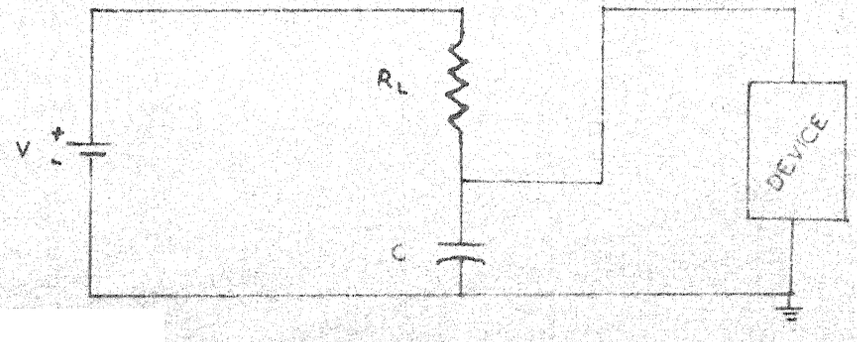

FIG. (2.2)

SIMPLE OSCILLATOR CIRQUIT USING CCNR DEVICE

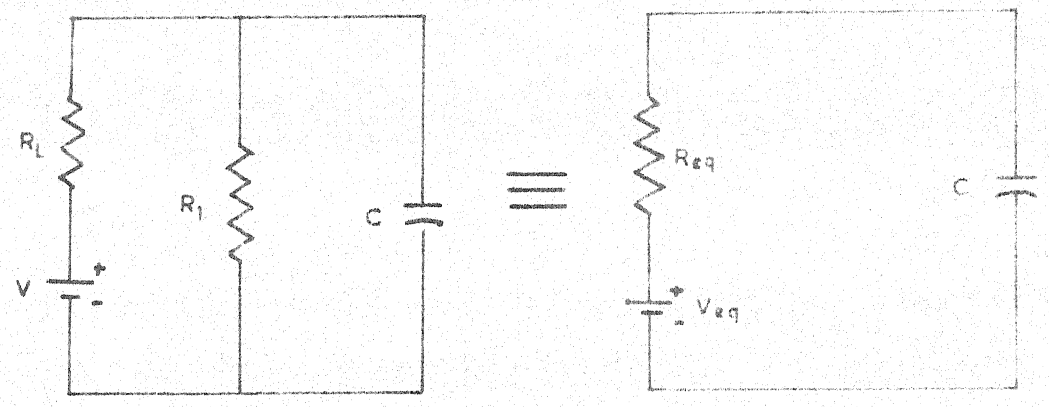

FIG. (23)
EQUIVALENT CIRCUIT FOR THE SEGMENT AB

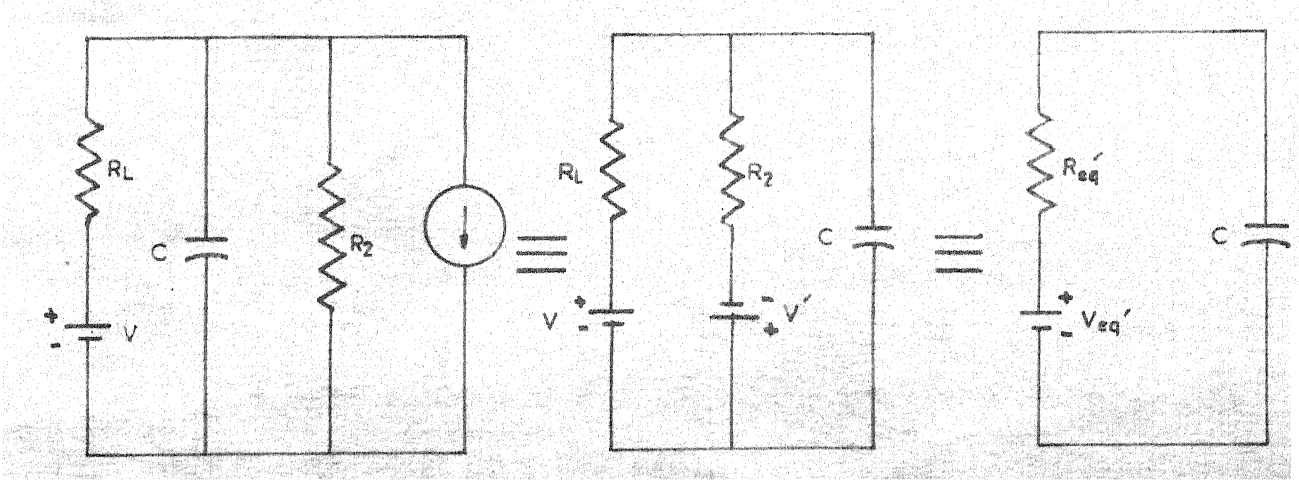

FIG. (24)
EQUIVALENT CIRCUIT FOR THE SEGMENT CD

2.3 Time Period

It can be seen that the circuit switches rather abruptly from B to C and from D to A. These switching times are relatively small and are neglected in the analysis.

When the operating point is traversing the segment AB, the device can be replaced by a simple equivalent circuit shown in Figure (2.3) and the time T_1, taken by the operating point to move from A to B is obtained as follows:

Let $V_{eq} = \dfrac{V \times R_1}{R_1 + R_L}$ and $R_{eq} = \dfrac{R_1 \times R_L}{R_1 + R_2}$ (2.1)

For a circuit with a single time constant,

$$v(t) = V_{final} + (V_{initial} - V_{final})e^{-t/\tau} \qquad (2.2)$$

where τ is time constant of the circuit.

With reference to Figure (2.1) set

$$V = V_v \text{ for } t = 0 \quad \text{and} \quad V = V_{eq} \text{ for } t = \infty$$

Thus

$$v(t) = V_{eq} + (V_v - V_{eq})e^{-t/CR_{eq}}$$

If the time taken for the operating point to traverse the segment AB is T_1, we can write

$$V_p = V_{eq} + (V_v - V_{eq})e^{-T_1/(CR_{eq})}$$

or

$$T_1 = CR_{eq} \times \ln\left(\frac{V_{eq} - V_v}{V_{eq} - V_p}\right) \qquad (2.3)$$

Similarly for the segment C_D, the device can be replaced by a resistance R_2 in parallel with a current source of magnitude I_o. The equivalent circuit of the device is shown in Figure (2.4).

Where

$$V' = I_o \times R_2, \quad V'_{eq} = \frac{VR_2 - V'R_L}{R_2 + R_L}$$

and

$$R_{eq}' = \frac{R_L * R_2}{R_L + R_2} \qquad (2.4)$$

Again using Equation §2.2) and setting

$$v = V_p \text{ at } t = 0 \quad \text{and} \quad v = V'_{eq} \text{ at } t = \infty$$

we get

$$v(t) = V'_{eq} + (V_p - V'_{eq})e^{-t/CR_{eq}'}$$

If T_2 is the time taken by the operating point to traverse the segment CD, we can write

$$v_v = V_{eq}' + (V_p - V_{eq}')e^{-T_2/CR_{eq}'}$$

or

$$T_2 = CReq' \ \ln\left(\frac{V_p - V_{eq}'}{V_v - V_{eq}'}\right) \qquad (2.5)$$

The period of oscillations $T = T_1 + T_2$ will be given by

$$T = CR_{eq} \ln\left(\frac{V_{eq} - V_v}{V_{eq} - V_p}\right) + CR_{eq}' \ln\left(\frac{V_p - V_{eq}'}{V_v - V_{eq}}\right) \qquad (2.6)$$

If a stable relaxation oscillator is to be obtained it will be necessary for the period to be insensitive to variation in the ambient temperature and variation in the supply voltage.

2.4 Effect of Variation of Supply Voltage

From Equation (2.3)

$$T_1 = CR_{eq} \ln \left(\frac{V_{eq} - V_v}{V_{eq} - V_p}\right)$$

If V_v and V_p are of the form

$$V_v = K_1V,\ V_p = K_2V \text{ and } V_{eq} = \frac{R_1v}{R_1+R_L} = K_3V,$$

$$T_1 = CR_{eq} \ln \left(\frac{K_3V - K_1V}{K_3V - K_2V}\right) = CR_{eq} \ln \left(\frac{K_3 - K_1}{K_3 - K_2}\right)$$

(2.6)

The value of V_{eq}' in terms of R_2, R_N, R_L, V_p, V_V and V is determined below.

From Figure (2.1) V_{eq}' is the point of intersection of lines representing R_1 and the loadline R_L. Equation for the load line R_L is

$$v = V - i \times R_L \qquad (2.8)$$

Now

$$I_v = \frac{V_p - V_V}{R_N} + \frac{V_P}{R_1}$$

Therefore Equation for the segment CD is given by

$$u = v_V + \left[1 - \left(\frac{V_p - V_V}{R_N} + \frac{V_p}{R_1}\right)\right] R_2 \qquad (2.9)$$

Solving Equation (2.8) and (2.9) simultaneously and eliminating i we get the value of V_{eq}'

$$V_{eq}' = V_v + \left[\frac{V - V_{eq}'}{R_L} - \frac{V_P - V_V}{R_N} + \frac{V_P}{R_1}\right] R_2$$

or

$$V_{eq}' = \frac{R_1}{R_2 + R_L}\left[V_v \frac{R_N + R_2}{R_N} - VP \frac{R_1 + R_N}{R_1 + R_N}\right] R_2 + \frac{V R_2}{R_N}$$

Since, R_2, R_N and R_L are fixed and V_V and V_P are proportional to supply voltage V, Veq' can be expressed as

$$Veq' = K_4 V$$

substituting for V_p,V_v and Veq' in Equation (2.5) we get

$$T_2 = CR_{eq}' \ln \frac{K_2 - K_4}{K_1 - K_4} \qquad (2.10)$$

Total time period from Equation (2.7) and (2.10)

$$T = T_1 + T_2$$

$$= CReq \ln \frac{K_3 - K_1}{K_3 - K_2} + CReq' \ln \frac{K_2 - K_4}{K_1 - K_4} \qquad (2.11)$$

If Req, Req' and C are constant it can be seen that supply voltage variation will not effect the period of oscillation.

2.5 Effect of Variation of Temperature

It is clear from Equations (2.6) (2.1), (2.4) that C, R_1 and R_2 should have a very low temperature coefficients to obtain a stable oscillator.

The maximum design of a circuit with a piece-wise linear i-v characteristics where V_p,V_V,R_1,R_2 and R_N are controlled extremally will now be discussed.

2.6 Basic Negative Impedance Convertor

A simple circuit configuration [3] is shown in Figure (2.5). The input current I forms the emitter current of the transistor T_1. A dependent current source ($I_{c2} = nI_{c1}$) whose magnitude is linearly related to the collector current of the transistor T_1 is obtained by the diode-transistor combination D_2, T_2. The arrangement where the diode is a diode connected transistor has temperature compensating features and is widely used in the integrated circuits. This combination is widely known as the current mirror. The additional diode connected transistor D_1 compensates for the voltage drop across the emitter-base junction of the transistor T_1, provided the transistors are identical and the current through diode D_1 is equal to the input current I. Under these conditions, the voltage across the input and output parts will be equal, resulting in current inversion type Negative Impedance Converter (NIC).

2.7 i-V Characteristics

The i-v characteristics of NIC, looking into node A can be studied by assuming a current I, flowing into the node A. Neglecting (for the time being), the voltage drops across the resistor R_H and the diode D_1 due to the leakage currents of the reverse-biased collector-base junctions of T_1 and T_2, the potential at the base of the transistor T_1 is V_p. As long as the voltage at

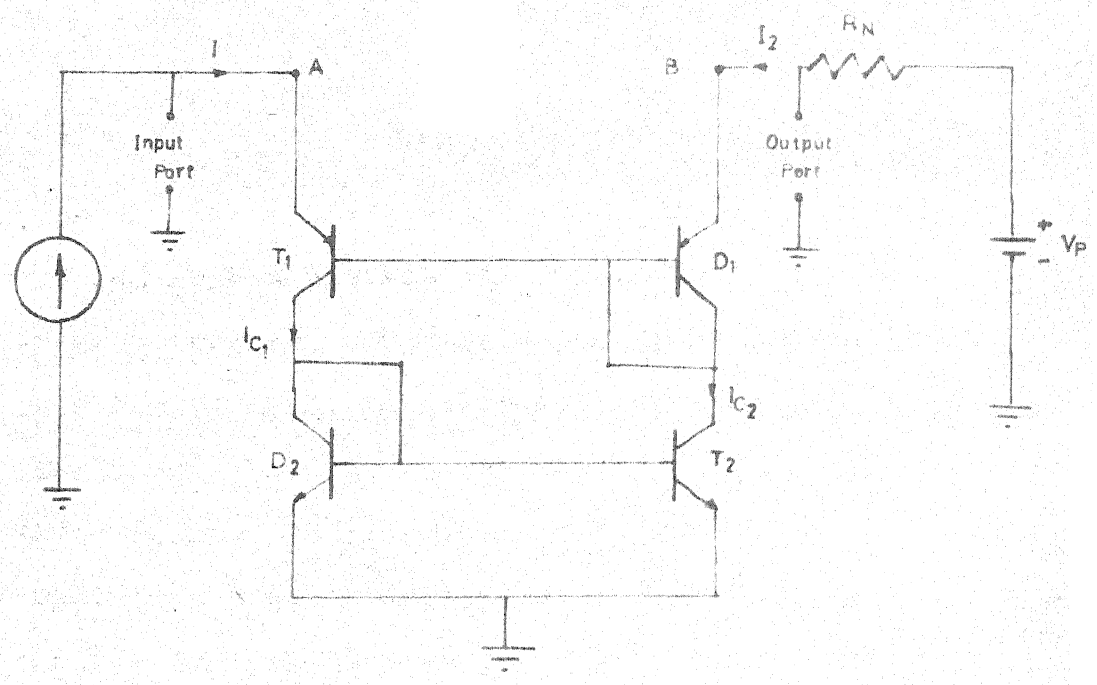

FIG. (2.5)
SIMPLE N I C CIRCUIT

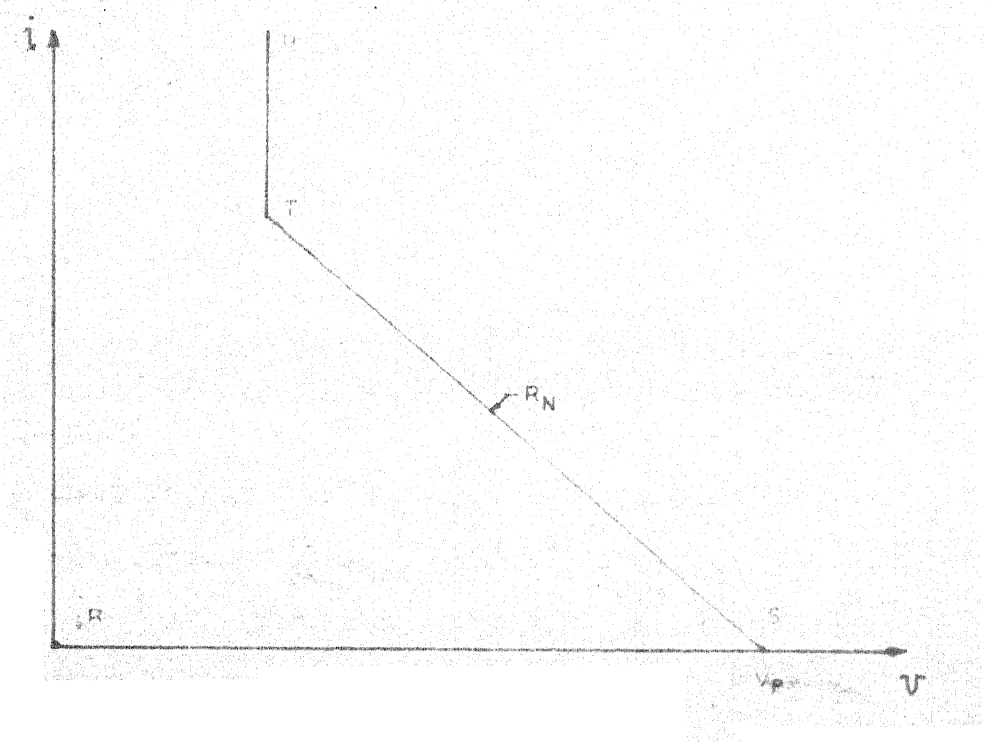

FIG. (2.6)
TERMINAL CHARACTERISTICS OF THE NIC

the node A is less than V_p, the emitter-base junction of the transistor T_1 is reverse biased and the transistor is cut off. Thus, except for leakage currents, there is no current flowing in the diode D_2 and hence no current flows in the transistor T_2 as well. Neglecting the reverse saturation current of the emitter-base junction of T_1, the i-v characteristics upto a voltage V_p is represented by the segement RS (Figure 2.6b).

When the voltage at the node A goes above V_p, the emitter-base junction of the transistor T_1 is forward biased and the collector current of T_1 flows through diode D_2 which turns on the transistor T_2.

If the diode-connected transistor D_2 and the transistor T_2 are matched then

$$\frac{I_{c2}}{I_{c1}} = \frac{\beta}{\beta+2} \qquad (2.12)$$

where β is common-emitter current gain of the npn transistors.

It is clear that as I is made to increase, I_2 increases proportionately. Since the voltage at node B is $(V_p - I_2 R_N)$, it continues to fall as $I_2(n/I_1)$ increases; till the transistors saturate. If equal currents flow through D_1 and T_1 and if D_1 and emitter-base junction of T_1 are matched, the voltage at the node A will be equal to voltage at node B.

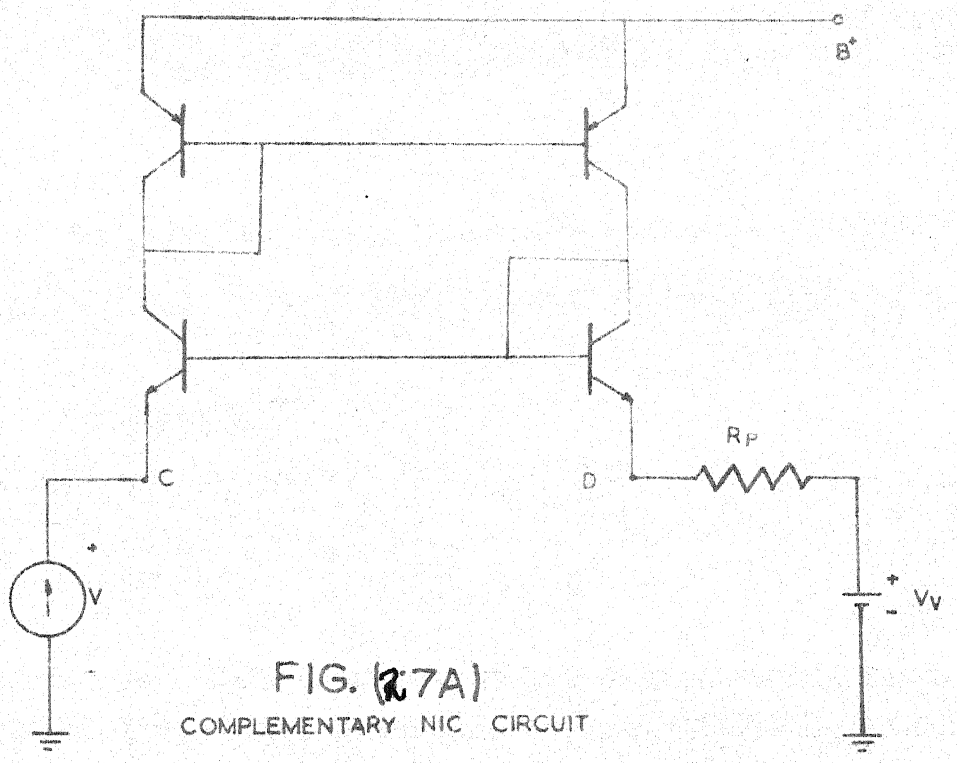

FIG. (7A)
COMPLEMENTARY NIC CIRCUIT

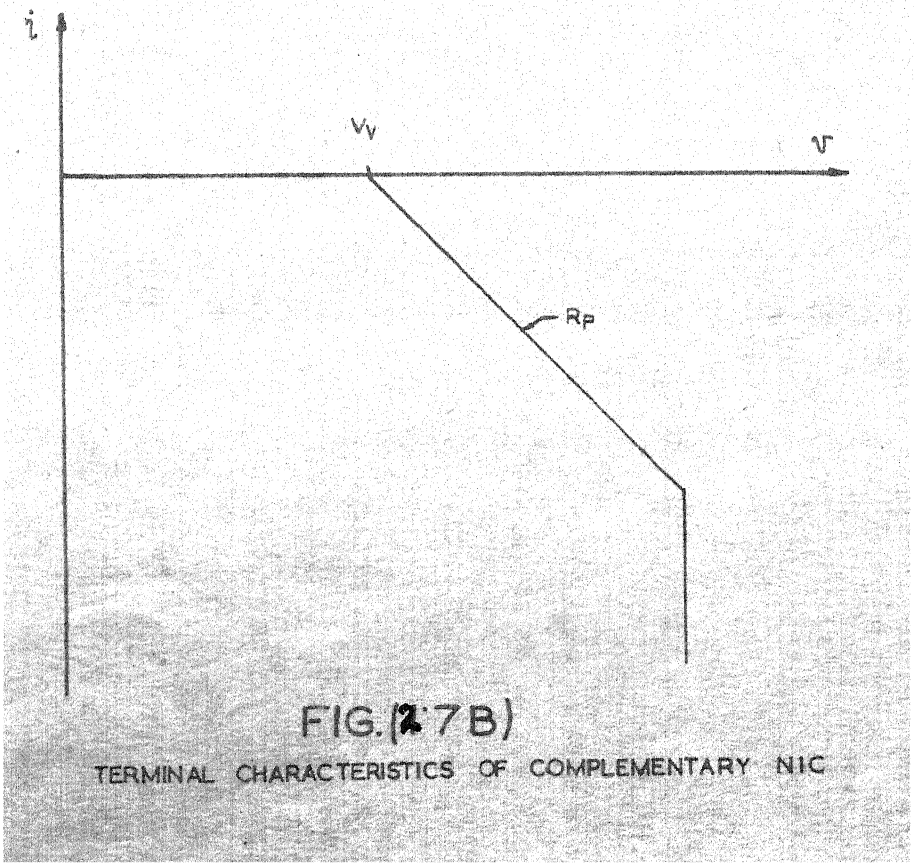

FIG. (7B)
TERMINAL CHARACTERISTICS OF COMPLEMENTARY NIC

Hence the i-v characteristics of the device after the transistors conduct are represented by segment STU (Figure 2.6B). If the base current of the transistors T_1 and T_2 are neglected, I_2 will be euqal to 1 and the resistance wi R_N will appear as a negative resistance of magnitude R_N at the input port.

A complementary circuit arrangement is shown in Figure (2.7A). It can be eqsily seen that, looking at the node C, the circuit will have the terminal characteristics given in Figure (2.7B).

2.8 Two Terminal Current-Controlled Negative Resistance Device

The circuits of Figures (2.6A) and (2.7A) can be combined as shown in Figure (2.8A) to obtain a current-controlled negative resistance (CCNR) device. It is assumed that $V_p > V_v$ and $R_N > R_p$.

2.9 i-v Characteristics

As I is increased from zero, circuit (2) remains cut off (V_p being greater than V_v) till the voltage at node B falls below V_v. As the input current is increased further the potential at nodes A and B will go below V_v and the circuit (2) becomes active and the net resistance (R) from node B is given by

$$R = \frac{-R_p \times R_N}{R_N - R_p} \qquad (2.13)$$

If $R_N > R_p$, R is a negative resitance which appears as a positive resitance at node A (Figure 2.8A).

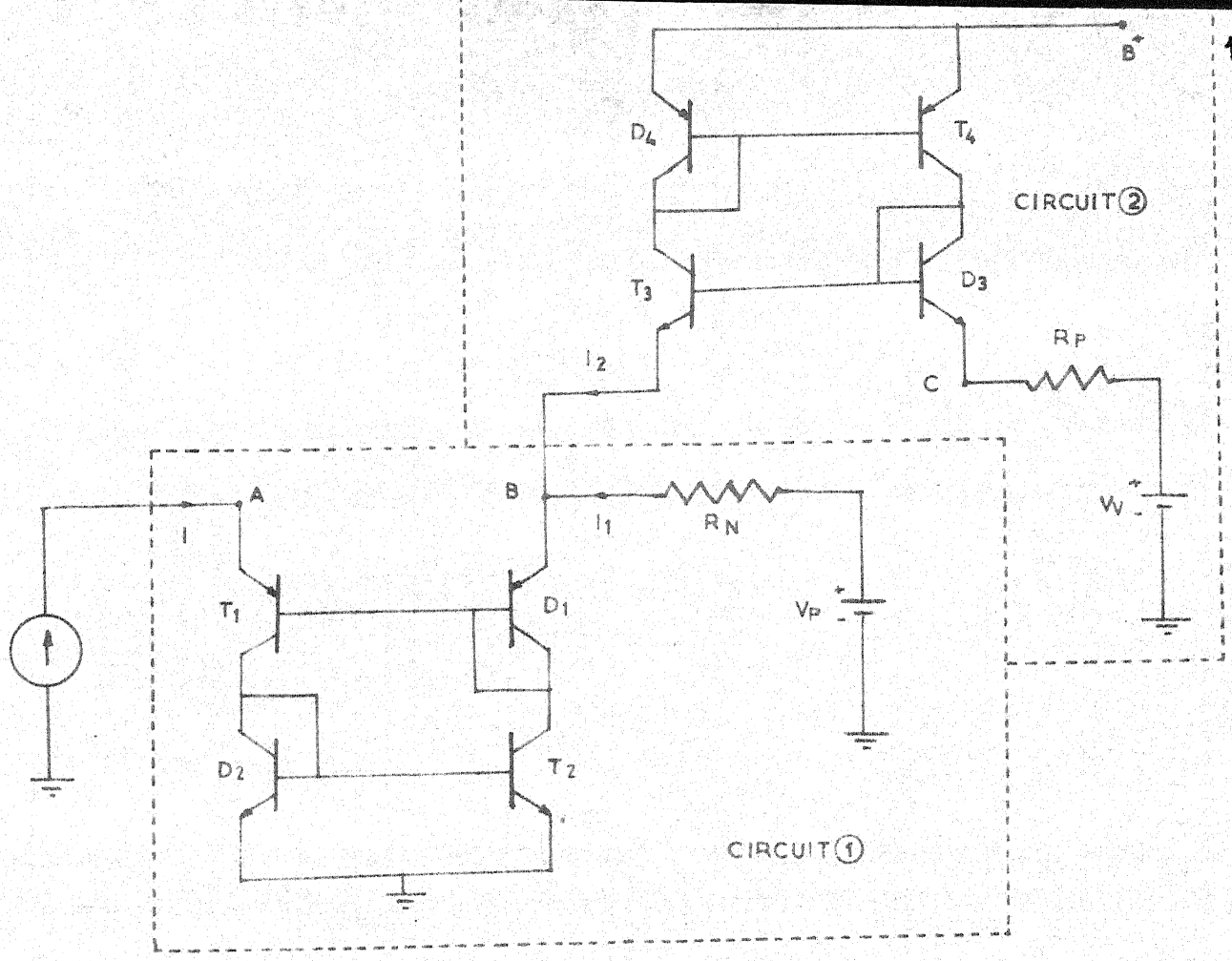

FIG. (2.8 A)

COMBINED CCNR CIRCUIT

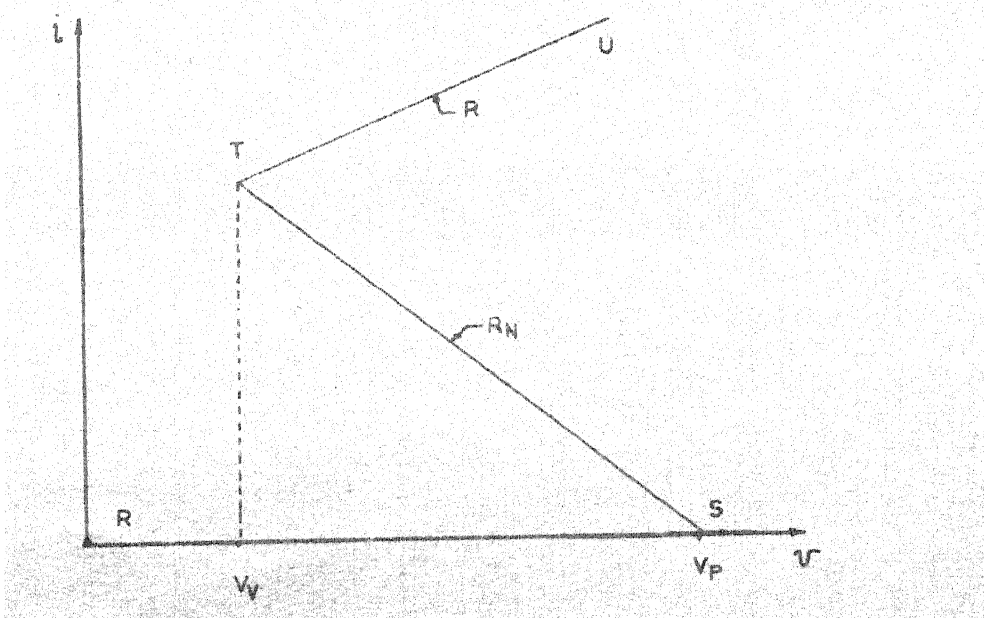

FIG. (2.8 B)

TERMINAL CHARACTERISTICS OF THE COMBINED CCNR CIRCUIT

The circuit, thus, will have the characteristics shown in Figure (2.8B).

CHAPTER 3

CIRCUIT REALIZATION

3.1 Choice of Devices

The CCNR device shown in Figure (3.1) was constructed with monolithic transistor arrays CA 3083 for npn transistors and CA 3084 for pnp transistors. These arrays provide matched devices on the same chip which ensure close thermal coupling and hence tracking of device parameters with temperature. The specifications of these are given in Appendix A. Precision metal film resistors are used to control the characteristics as well as defining V_p and V_v.

3.2 Overshoot Around Vp

In our earlier qualitative description of the circuit behaviour given in Section 1.31, we had neglected the leakage currents as well as the base currents of the transistors. Now we shall examine the influence of these currents.

With reference to Figure (3.2A) the reverse saturation current I_{CO1} and I_{CO2} of the collector-base junctions of the transistors T_1 and T_2 flow as shown explicitly in the figure. The sum of these currents flow in the diode D_2. This results in an equal emitter current in T_2. The corresponding collector current as well as $(ICO_1 + I_{CO2})$

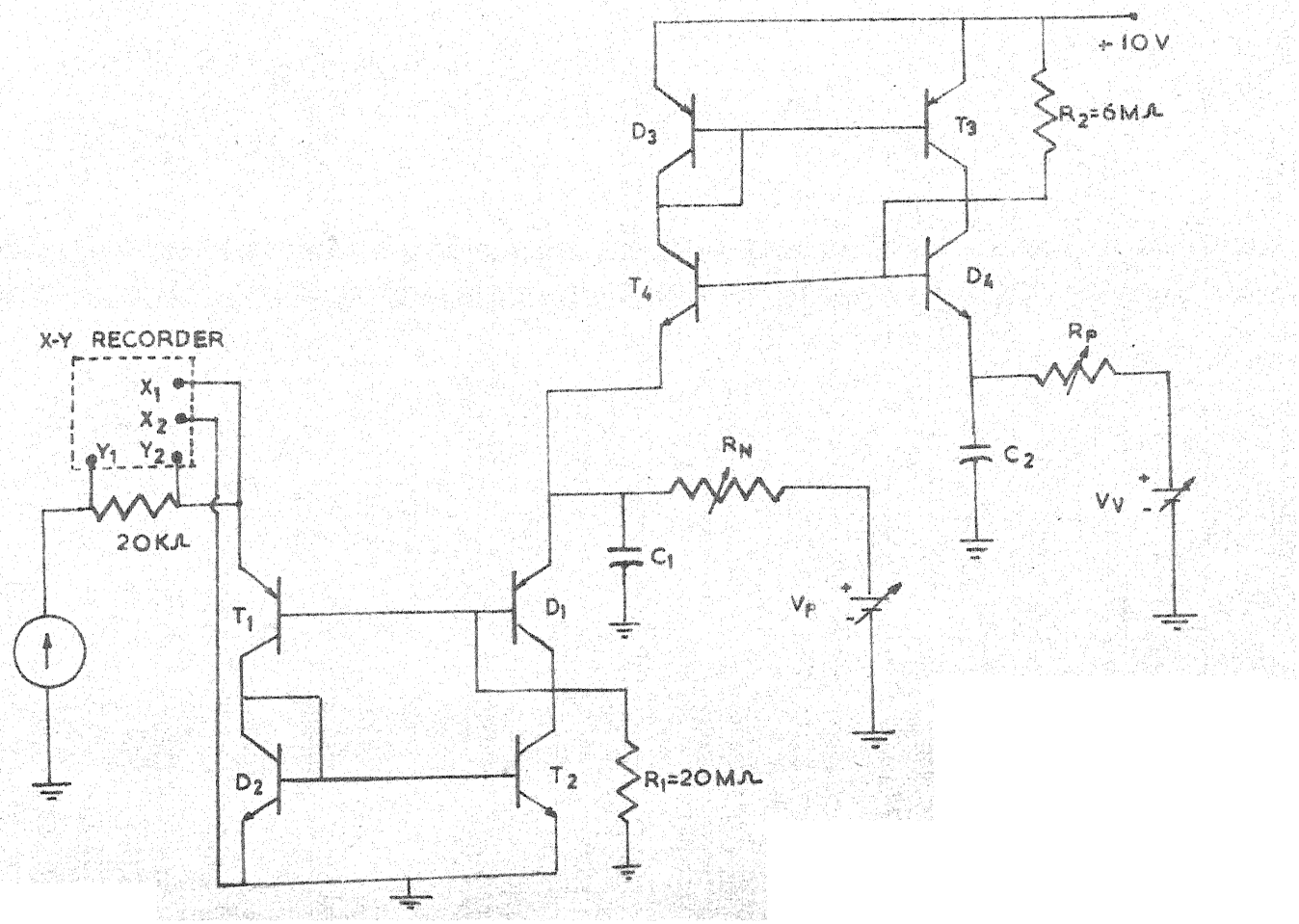

FIG. (3.1)

CIRCUIT REALIZATION USING TRANSISTOR ARRAYS

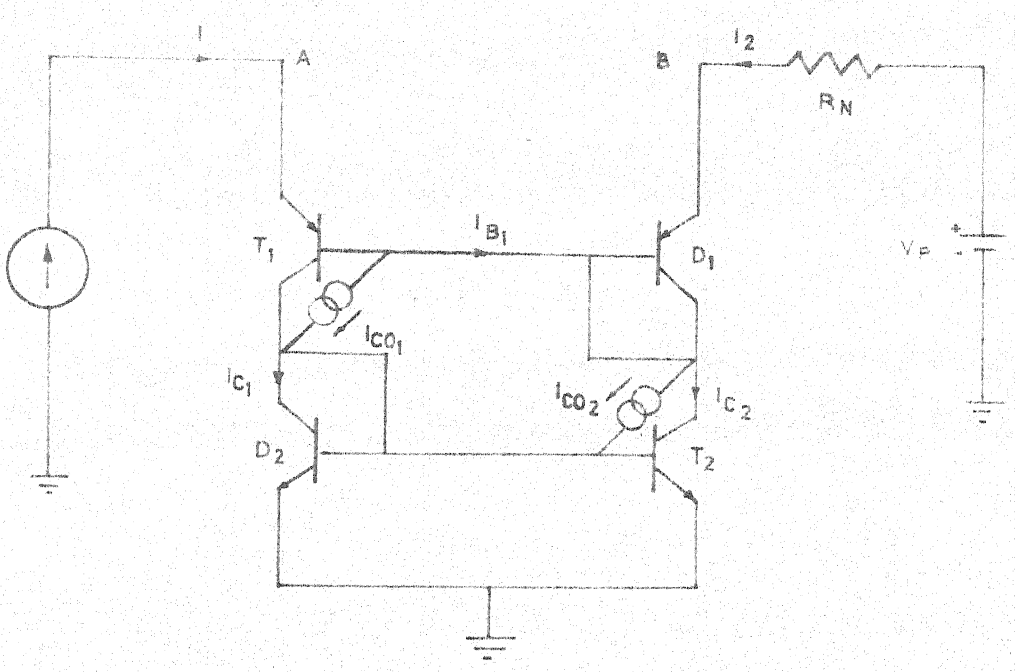

FIG. (3·2A)

INFLUENCE OF BASE CURRENTS AND I_{CO_1} AND I_{CO_2}

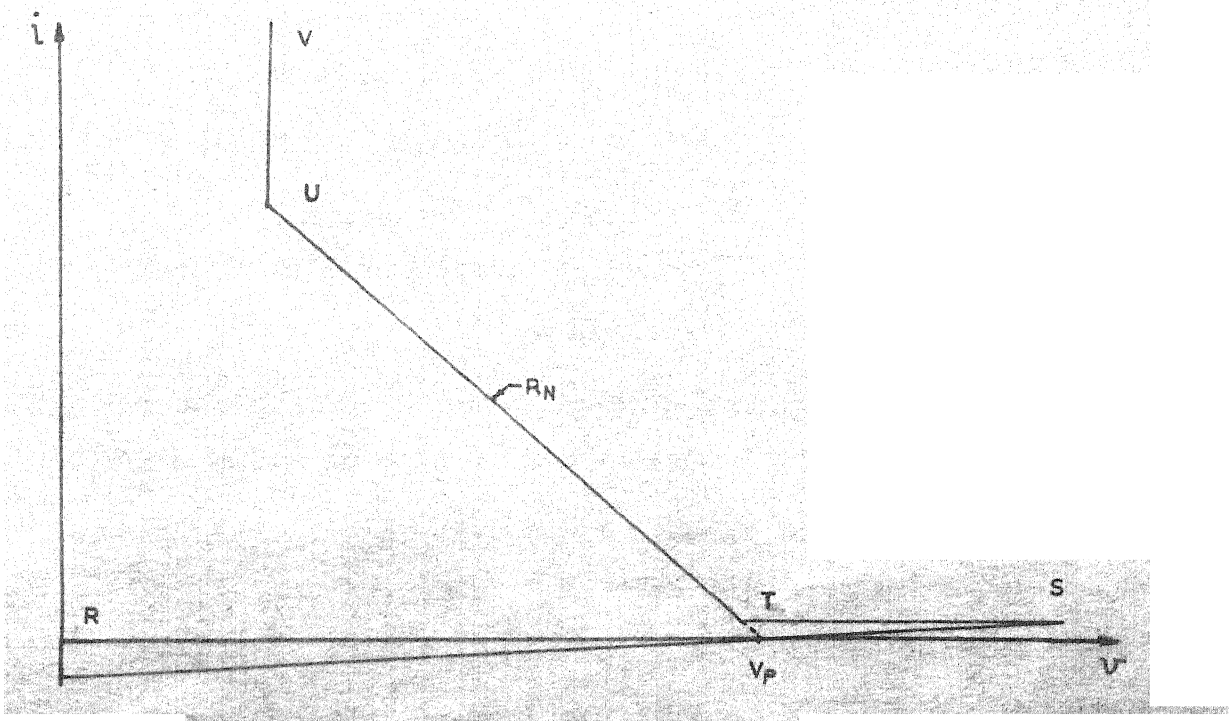

FIG. (3·2B)

PRACTICAL CHARACTERISTICS SHOWING OVERSHOOT AROUND V_P

flow through D_1 forward-biasing it slightly. When the voltage at the node A reaches a value when the transistor T_1 just starts conducting, its α is low and hence under these conditions the base current of T_1 tends to be large proportion and very little collector current would flow. Thus if I_{B1} is greater than IC_2, the diode D_1 will be reverse biased making the input voltage increase beyond V_p. As the input current I increases, the α of T_1 improves, so that eventually I_{B1} becomes equal to I_{C2} (Figure 2.2A). Beyond this point the diode D_1 will be forward biased and the circuit will operate as explained in Section 1.21. In other words, the practical characteristics will be as shown in Figure (2.2B).

A large resitance R_1 (chosen experimentally) is connected as shown in Figure (2.1) which will slightly forward bias the diode D_1 so that for low values of I, the diode D_1 never gets a chance to get reverse biased. This removes the over-shoot in the characteristics beyond V_p. Similarly the resistor R_2 removes the overshoot around the valley point.

3.3 Stabilization and Experimental Arrangement

It is well known [5] that small stray capacitances introduced between the node A and ground (due to test equipment connected at the node A) will make the circuit unstable. A simple way of stabilizing the circuit for plotting terminal i-v characteristics is to connect capacitors C_1 and C_2 as shown in Figure (3.1). The plots are obtained using the arrangement shown in Figure

(3.2C) and applying slowly varying currents so as to meet the quasi-static condition which makes the capacitor currents due to C_1 and C_2 negligibly small.

3.4 Effect of Variation of V_p and V_v

The peak voltage can be controlled by the variable power supply V_p, whown in Figure 3.1. Experimental results obtained by varying V_p are shown in Figure (3.3).

Similarly, valley voltage is controlled by varying variable power supply V_v and Figure (3.4) shows the experimental results.

3.5 Effect of Variation of R_N

The slope of the negative resistance region can be varied by changing the value of R_N (Figure 3.5). The value of negative resitance as measured from the i-v characteristics is in agreement with that predicted by Equation 1.12.

3.6 Effect of Variation of R_p

The slope of the positive resistance region of i-v characteristics can be controlled by varying R_p. Experimental evidence to this effect is shown in Figure 3.6.

It is observed that the characteristics are non-linear in this region. It is due to the reason that transistor T3 (Figure 2.1) is a lateral pnp device with low β, (of the order of 10), therefore the gain of the current mirror is highly β dependent. Since β of the transistor varies with current level as well as the collector-base reverse bias voltage, the current gain $\frac{I_1}{I_2}$ is not constant and hence the i-v characeristics are non-linear in this region. For smaller values of R_p the

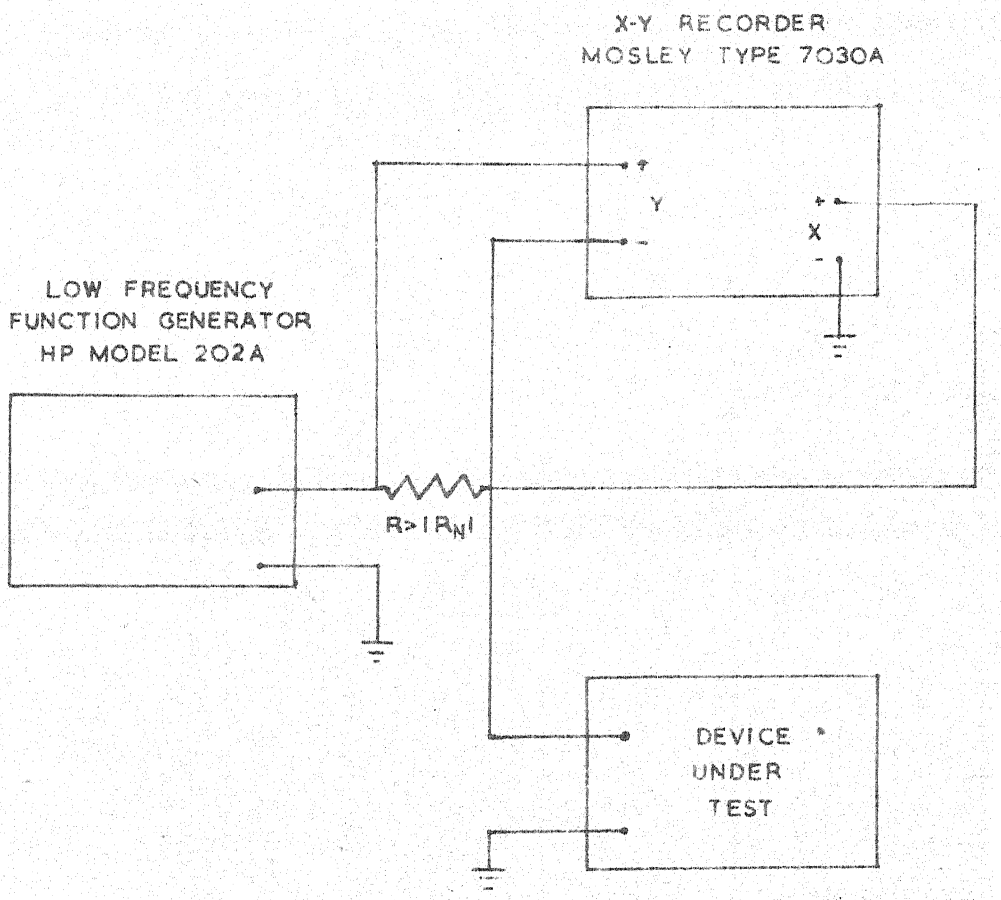

FIG. (3·2C)

EXPERIMENTAL ARRANGEMENT FOR CIRCUIT REALIZATION

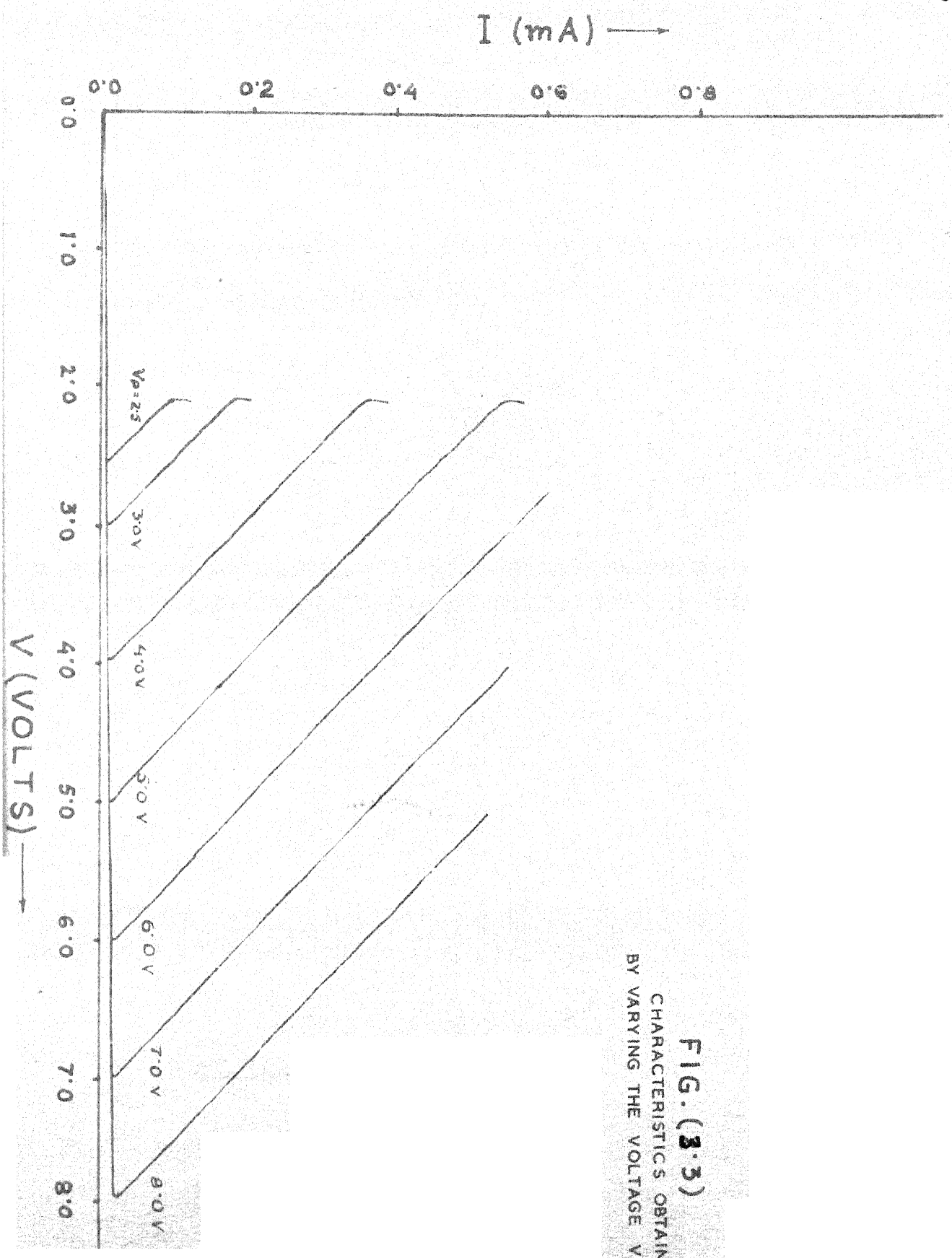

FIG. (3·3)

CHARACTERISTICS OBTAINED BY VARYING THE VOLTAGE V_P

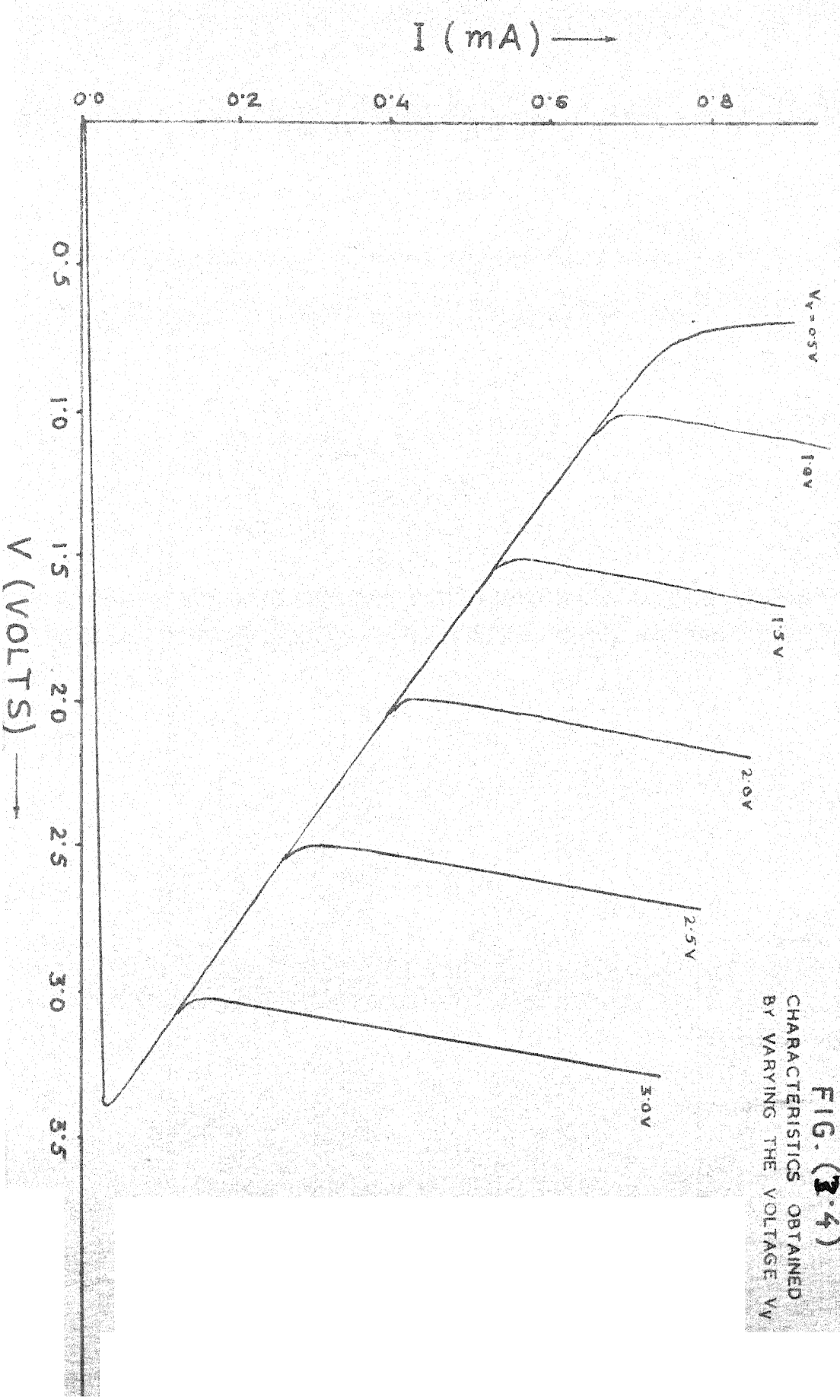

FIG. (2·4)
CHARACTERISTICS OBTAINED BY VARYING THE VOLTAGE V_Y

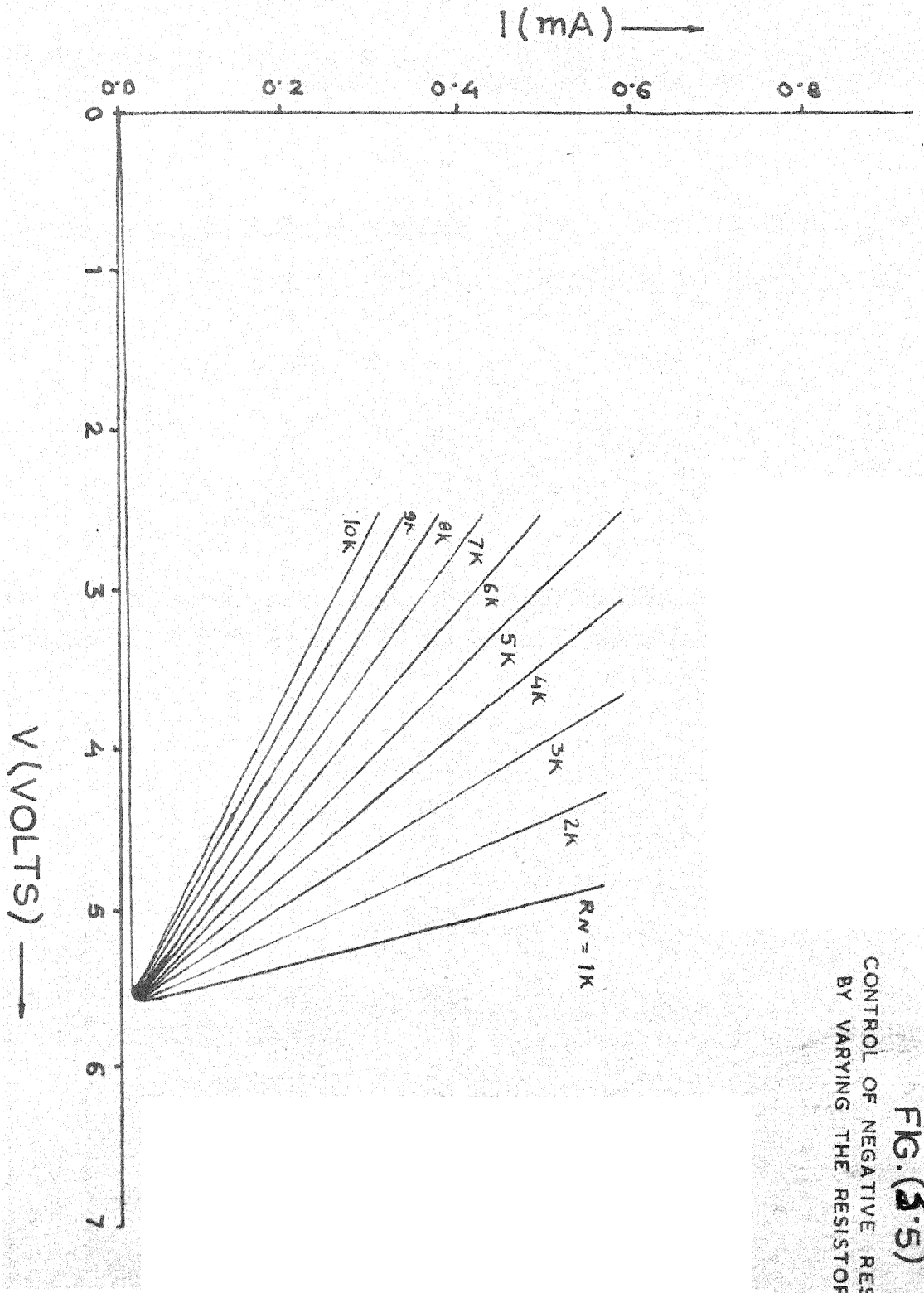

FIG. (3.5)

CONTROL OF NEGATIVE RESISTANCE BY VARYING THE RESISTOR R_N

FIG. (3·6)

CONTROL OF POSTIVE RESISTANCE REGION CD
BY VARYING THE RESISTOR R_P

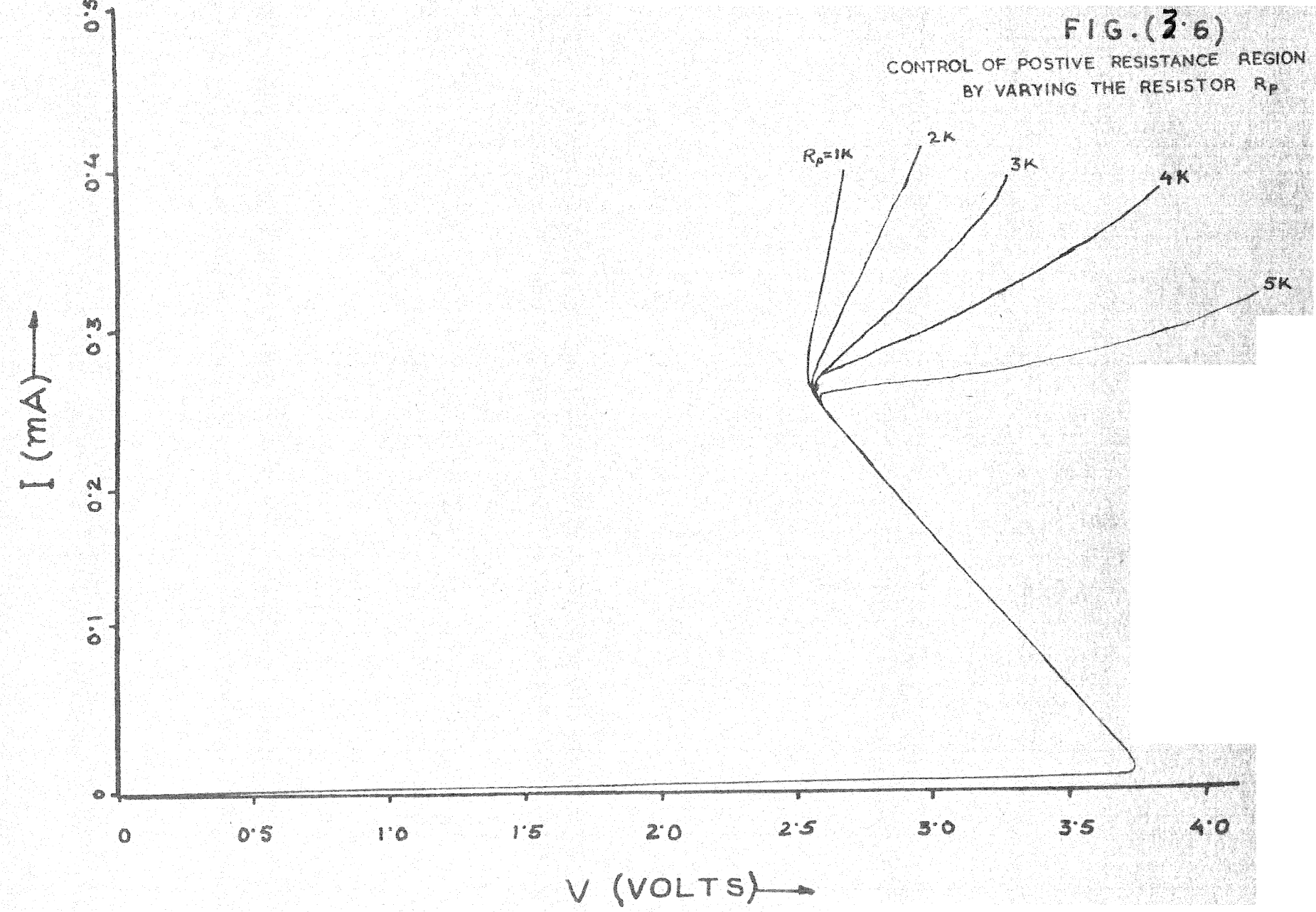

voltage variation is small resulting in less non-linearity. One method to reduce the β dependence of current gain and to increase the output impendance, is to use the Wilson's current mirrors [4] shown in Figure (3.7). This will have a current gain given by

$$\frac{I_1}{I_2} = 1 + \frac{2}{\beta^2 + 2\beta} \qquad (3.1)$$

The complete circuit employing Wilson's current mirrors is shown in Figure (3.8). The i-v characteristics of this circuit are found to be quite linear as seen from the experimental results shown in Figures 3.9, 3.10, 3.11, 3.12.

3.7 Effect of temperature Variation

Since the current gain of the mirrors is β dependent and β varies with temperature; even if R_N and R_P were held constant, the input resistance looking into node A (Figure 3.13) is slightly temperature sensitive. This is investigated experimentally by raising the temperature of the circuit of Figure (3.8) using an oven. The characteristics (Figure 2.14) show small changes of the order of 0.1%/°C in R_N and R_P.

With reference to Figure (3.8), the current gains

$$\frac{I_1}{I_2} = 1 + \frac{2\beta_1\beta_3 + 2\beta_5\beta_3 - 2\beta_1\beta_5 + 2\beta_1 + 4\beta_3 + 4}{\beta_1\beta_3\beta_5 + 2\beta_1\beta_5 - 2\beta_3 - \beta_3\beta_5 - 2} \qquad (3.2)$$

and

$$\frac{I_3}{I_4} = 1 + \frac{2\beta_9\beta_6 + 2\beta_8\beta_6 - 2\beta_9\beta_8 + 2\beta_9 + 4\beta_6 + 4}{\beta_9\beta_8\beta_6 + 2\beta_9\beta_8 - 2\beta_6 - \beta_8\beta_6 - 2} \qquad (3.3)$$

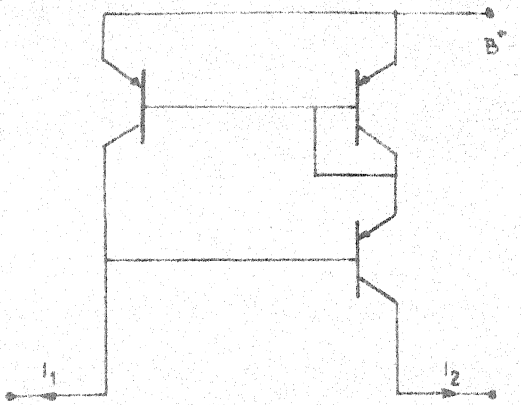

FIG. (3.7A)
WILSON CURRENT MIRROR

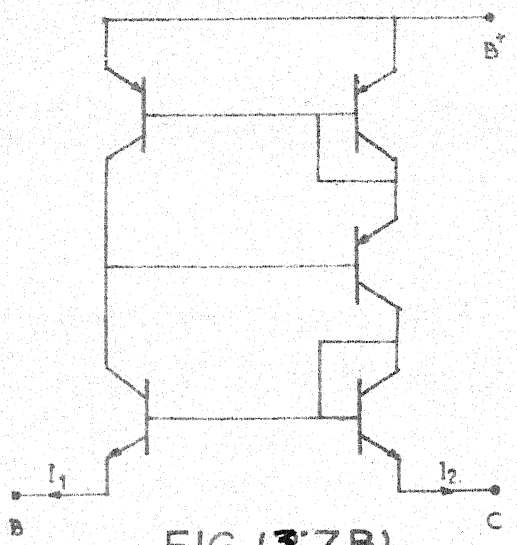

FIG. (3.7B)
NIC USING WILSON CURRENT MIRROR

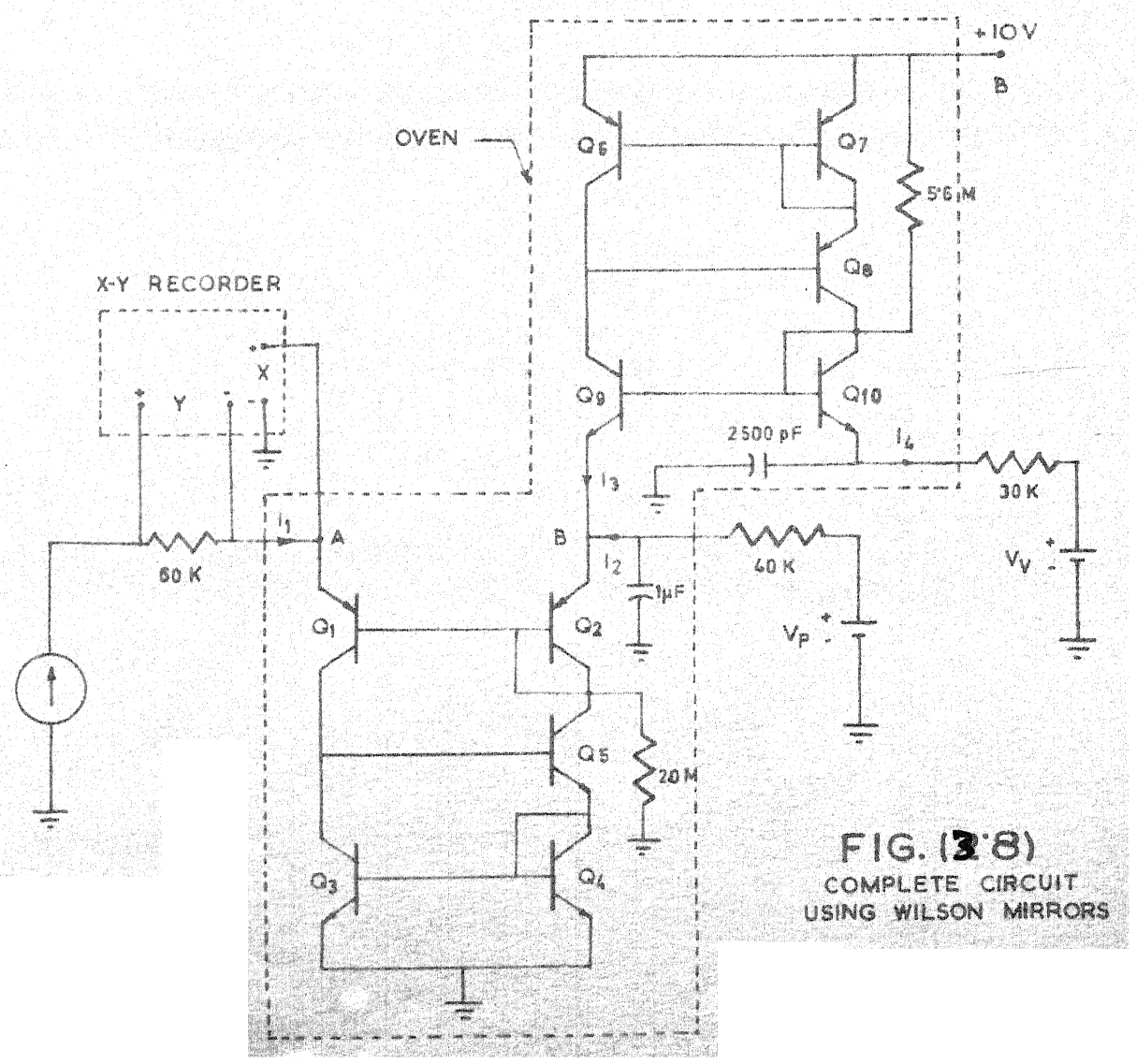

FIG. (3.8)
COMPLETE CIRCUIT
USING WILSON MIRRORS

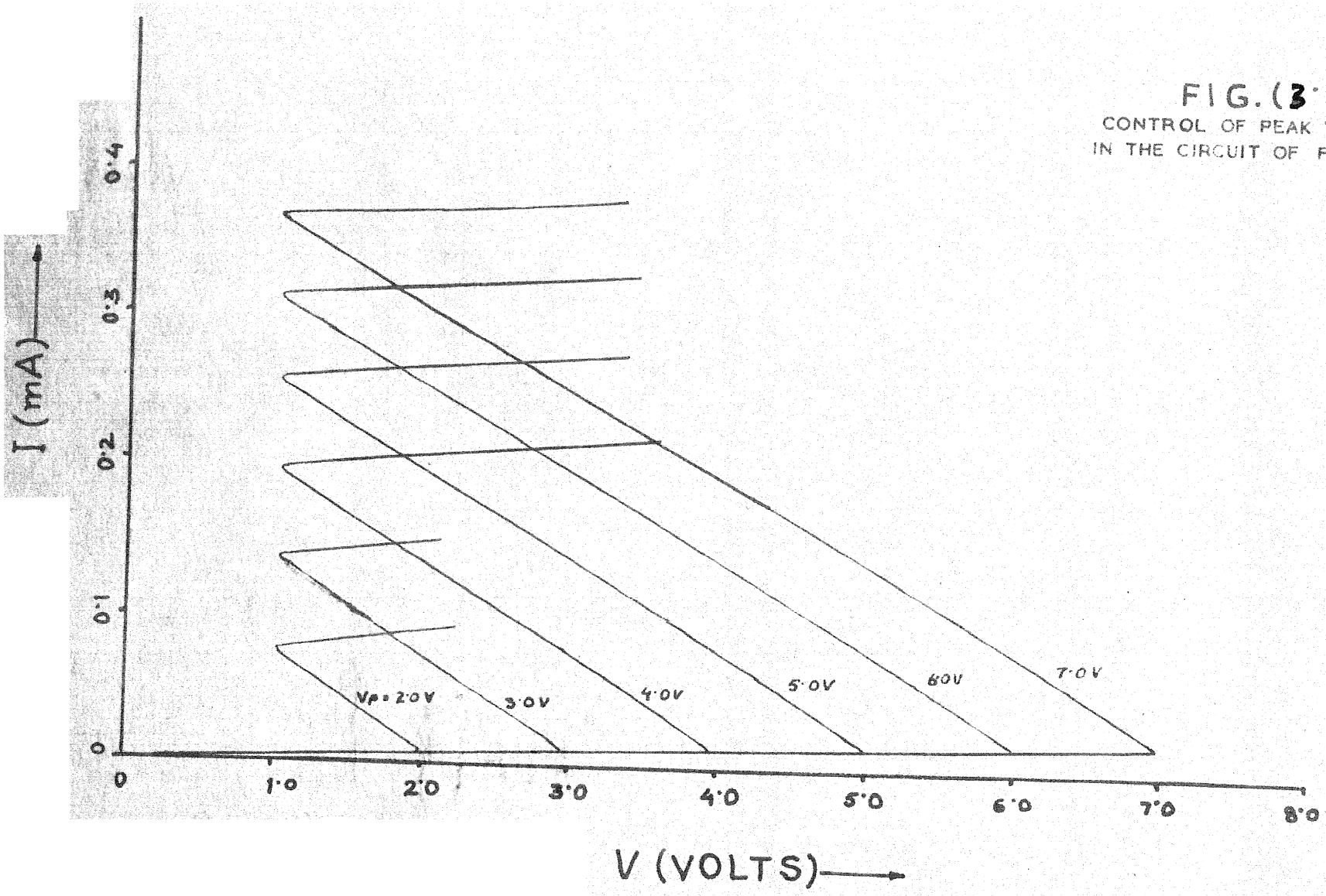

FIG. (3·9)
CONTROL OF PEAK VOLTAGE
IN THE CIRCUIT OF FIG. (2·8)

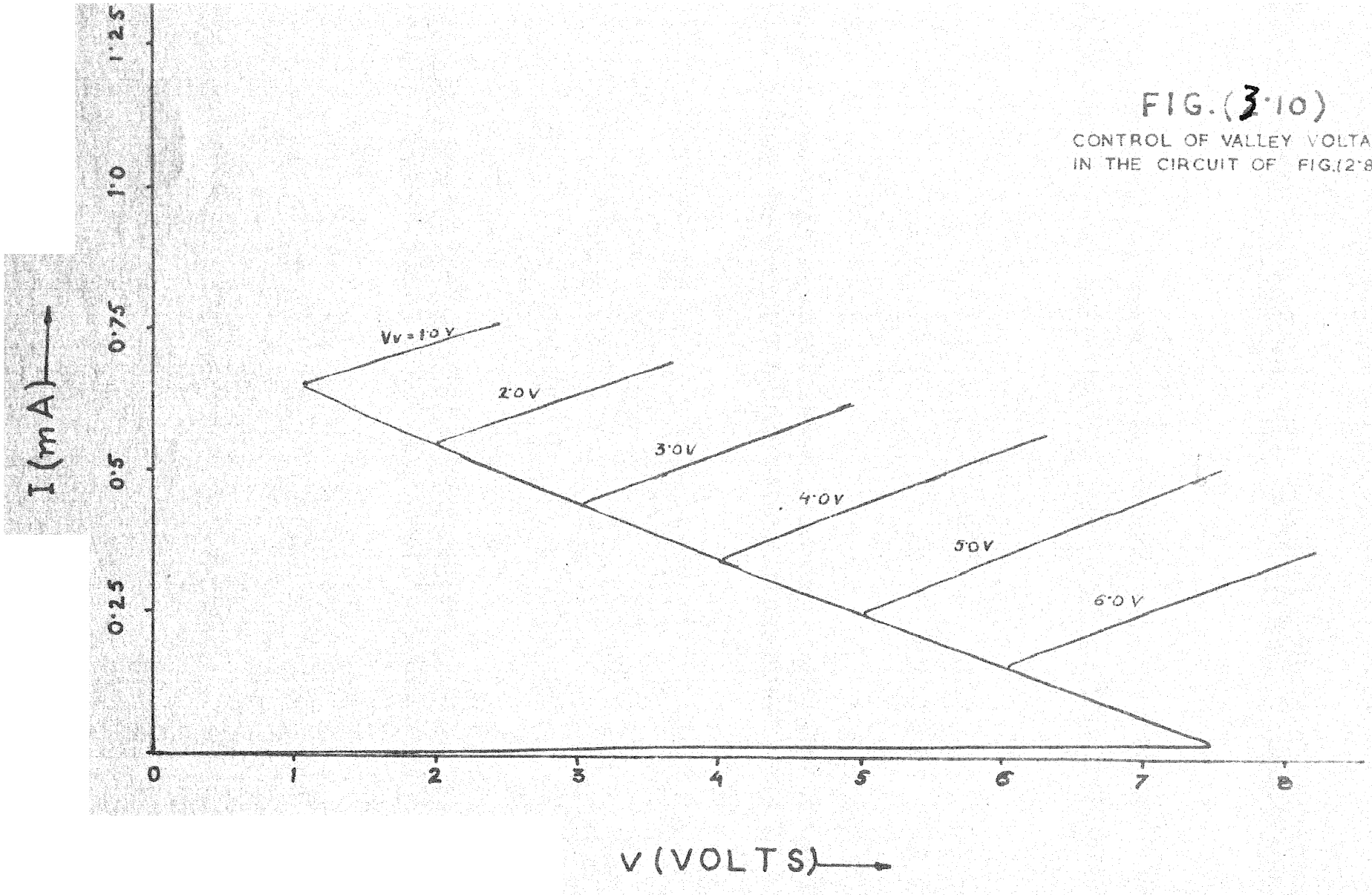

FIG. (3·10)
CONTROL OF VALLEY VOLTAGE
IN THE CIRCUIT OF FIG. (2·8)

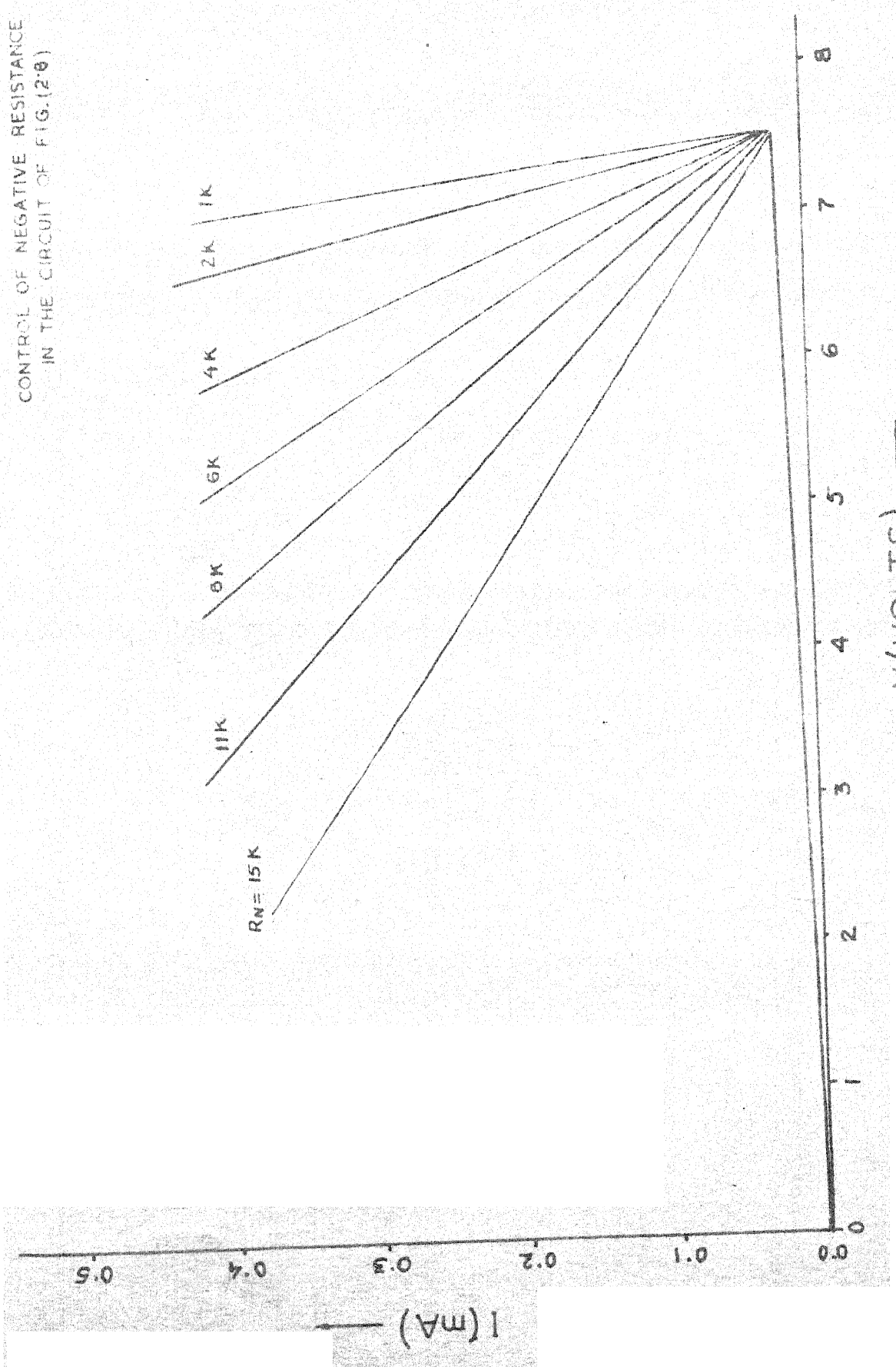

FIG. (3'11)

CONTROL OF NEGATIVE RESISTANCE
IN THE CIRCUIT OF FIG.(2'8)

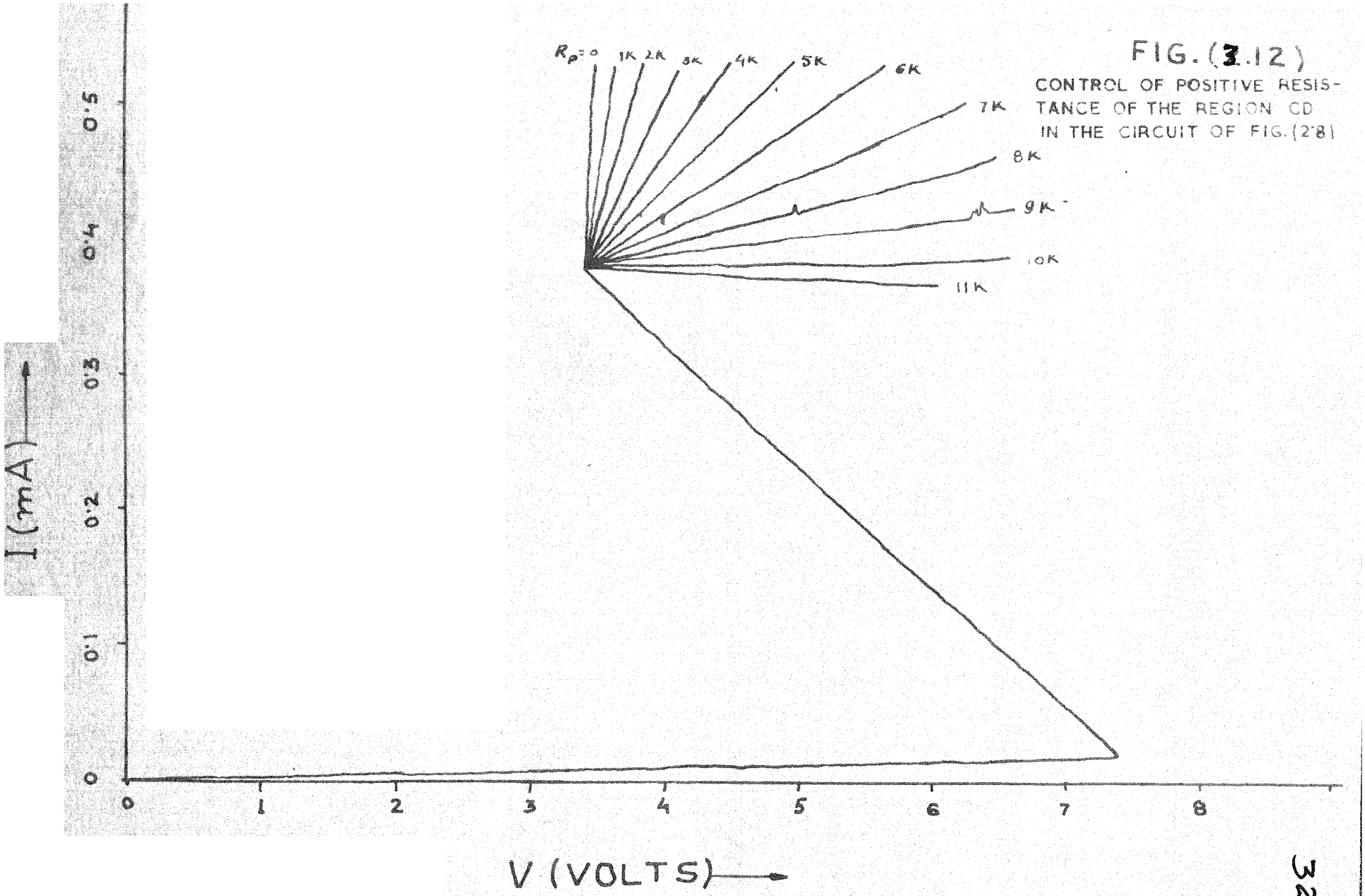

FIG. (3.12)
CONTROL OF POSITIVE RESISTANCE OF THE REGION CD IN THE CIRCUIT OF FIG. (2·8)

FIG.(3·14)

EFFECT OF TEMPERATURE VARIATION ON TERMINAL CHARACTERISTICS OF CIRCUIT SHOWN IN FIG.(2·8)

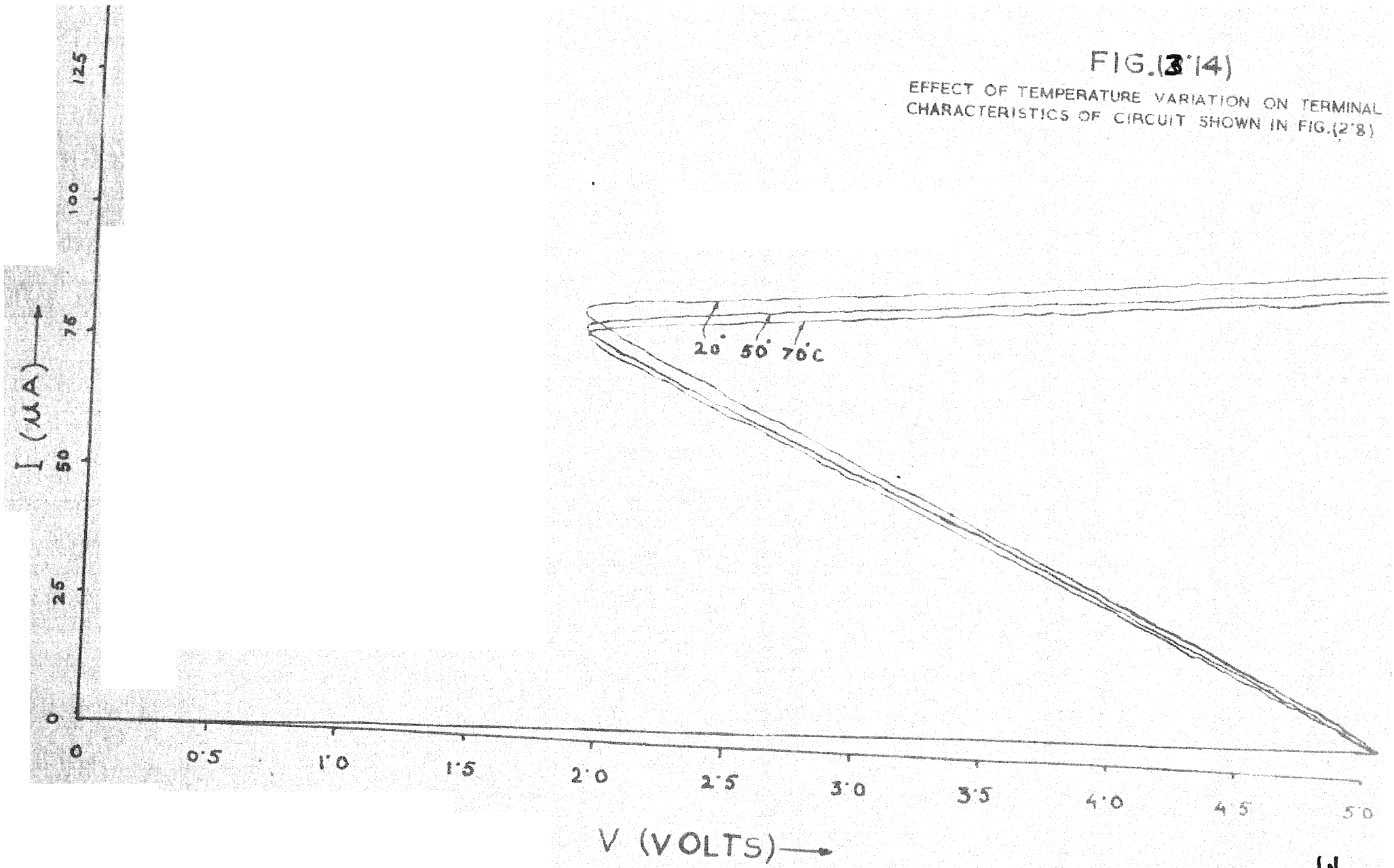

where the subscripts pertain to the respective transistors. If the current gain of all npn transistors is considered to be equal (β_n) and the gain of all pnp transistors is considered to be equal (β_p) also if it is assumed that gain of transistors Q_1 and Q_9 tends to infinity the Equation (3.2) and (3.3) will reduce to

$$\frac{I_1}{I_2} = 1 + \frac{2}{\beta_n^2 + 2\beta_n}$$

and

$$\frac{I_3}{I_4} = 1 + \frac{2}{\beta_p^2 + 2\beta_p}$$

Thus under the above conditions, the current gain is less β depedent than predicted by Equation (3.2) and (3.3). The temperature sensitivity is expected to be of the order of 90 p.p.m. taking the typical values (from the specification sheets) of β_n and variation of β_n with change in temperature from 25°C to 70°C.

Further improvement is investigated by increasing the current gain by Darlington connection of transistors Q_1, Q_2, Q_9 Q_{10}. The modified circuit is shown in Figure (2.15). It is seen from the i-v characteristics of circuit 1, of Figure 2.15 (Figure 2.16) that the conversion of R_N into an equivalent negative resistance is quite temperature insensitive.

To obtain a temperature independent conversion factor of unity the gain of the mirror should be unity. This can be achieved by adding resistors R_3 and R_4 (shown dotted in Figure 2.15) and adjusting them to obtain unity gain.

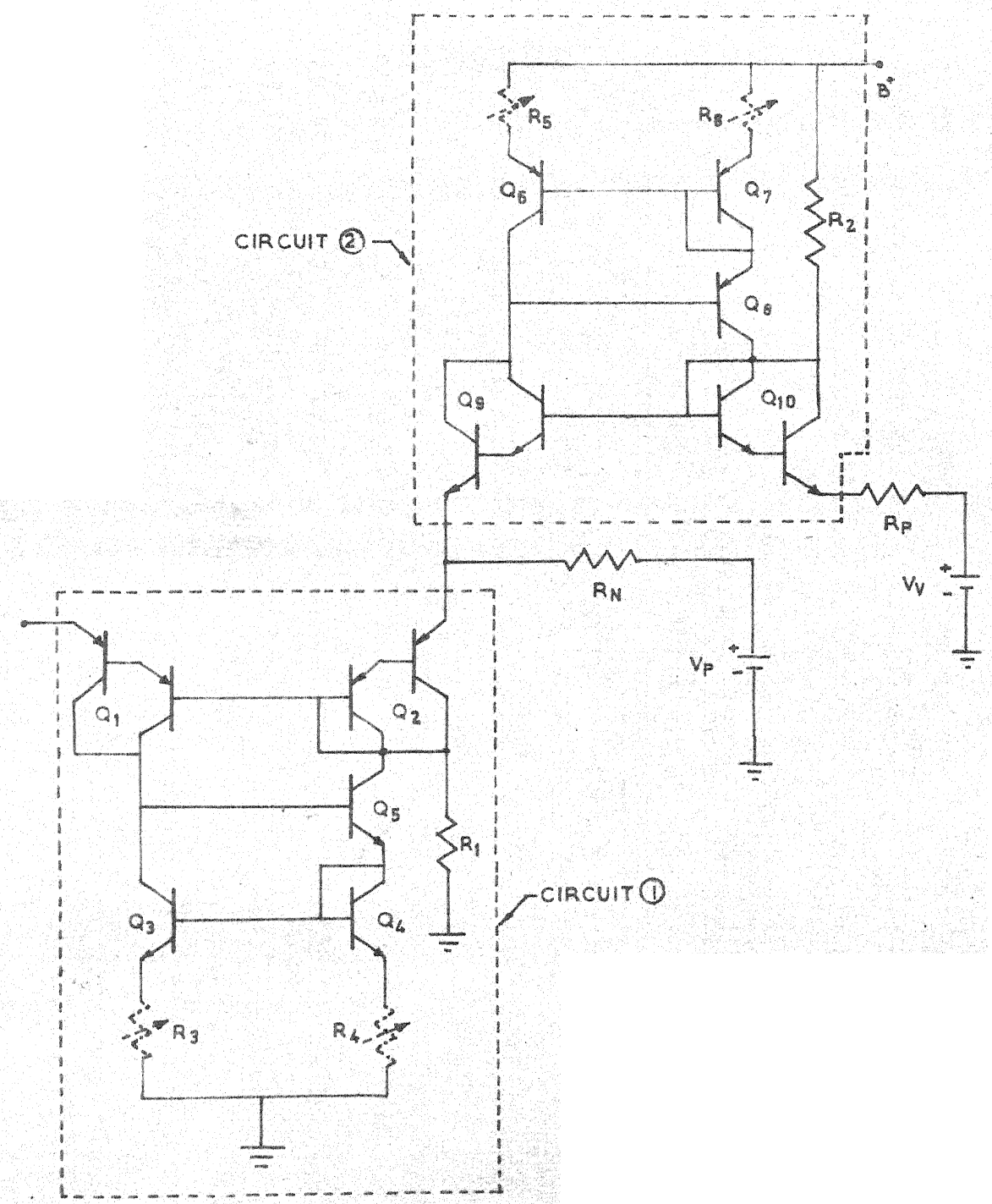

FIG. (3'15)

CIRCUIT CONTAINING DARLINGTON CONNECTED TRANSISTORS

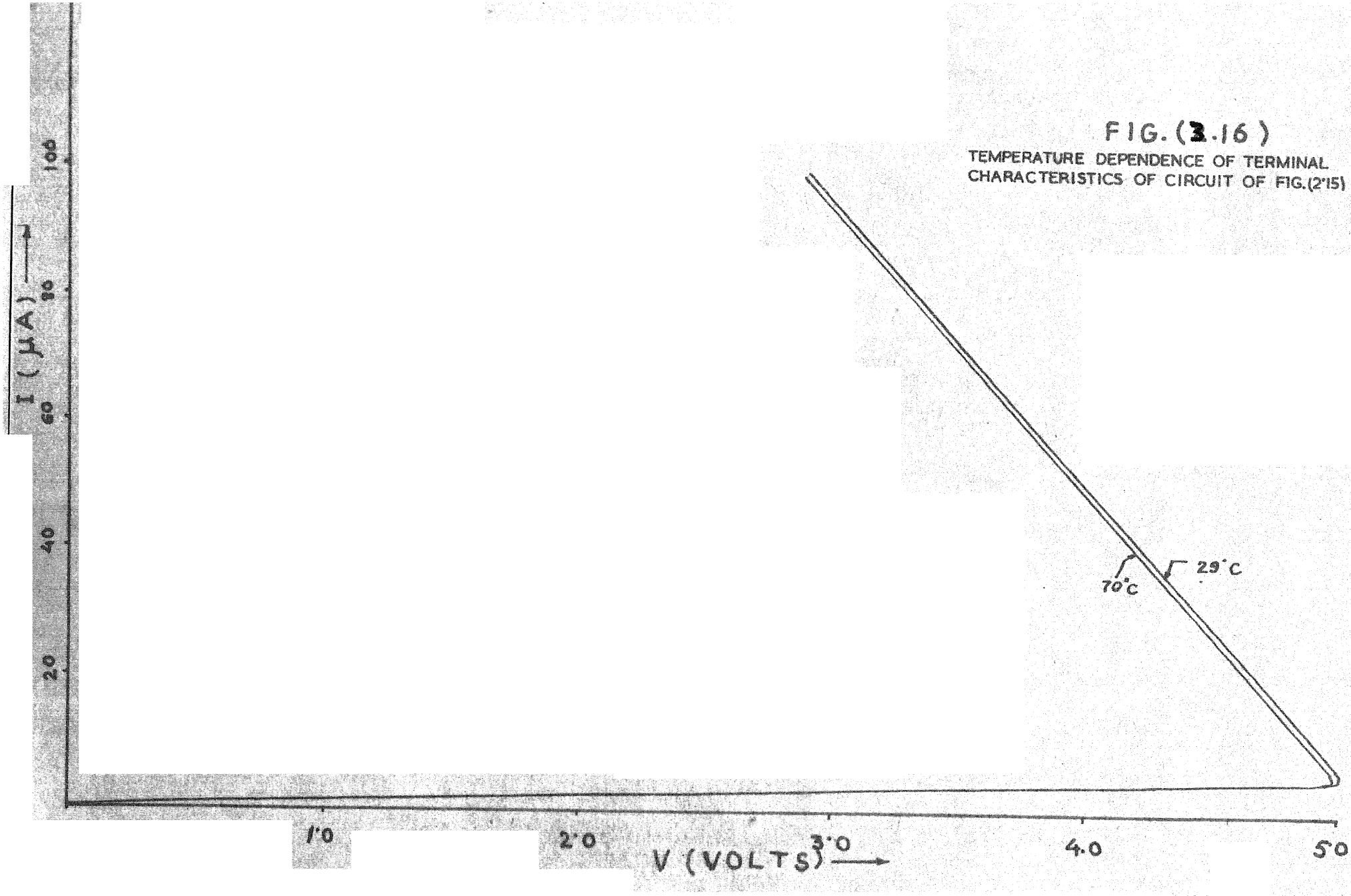

FIG. (3.16)
TEMPERATURE DEPENDENCE OF TERMINAL CHARACTERISTICS OF CIRCUIT OF FIG.(2'15)

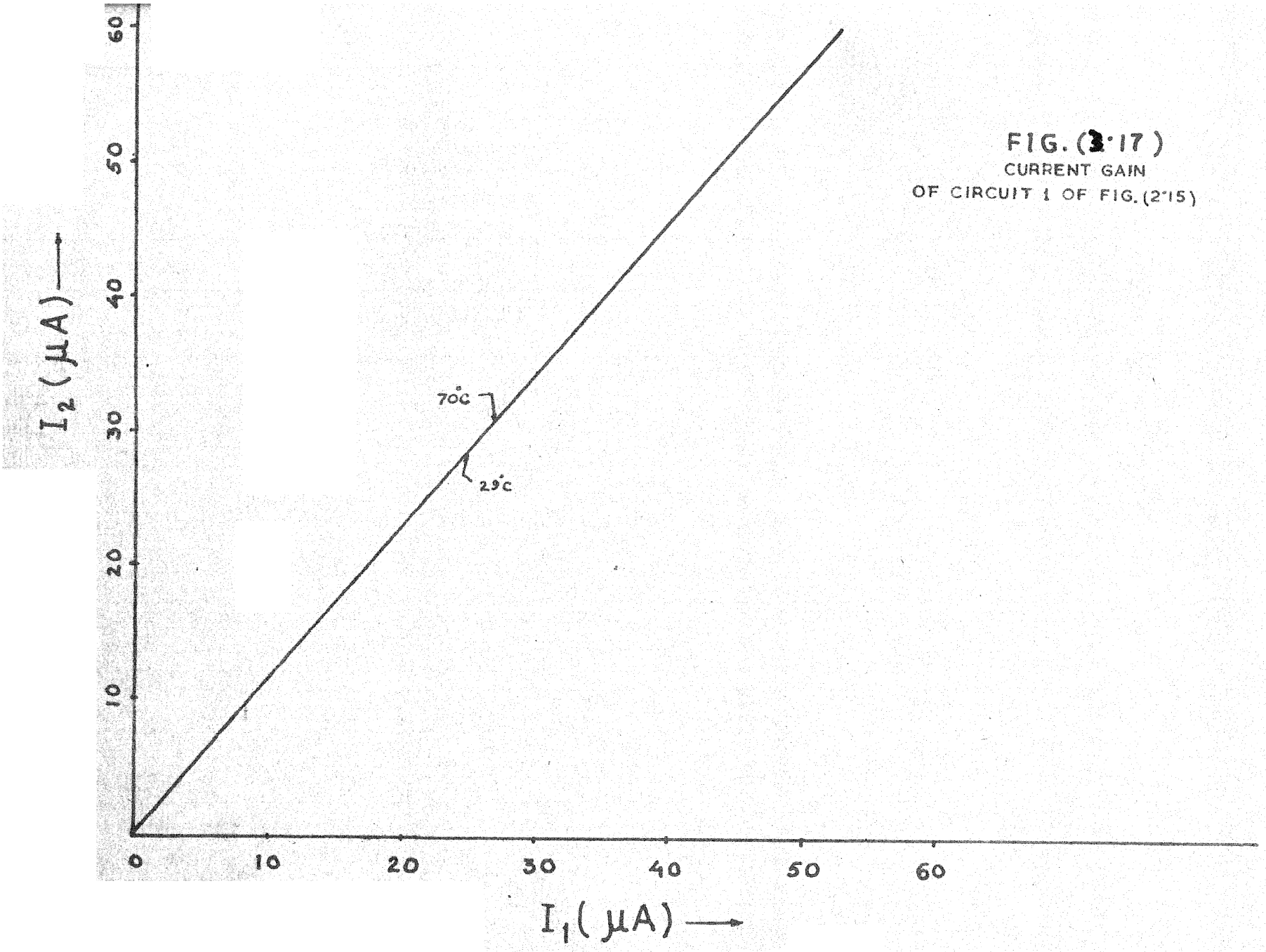

FIG. (3·17)
CURRENT GAIN
OF CIRCUIT 1 OF FIG. (2·15)

A similar modification and adjustment is done in the circuit 2.

CHAPTER 4

OSCILLATOR PERFORMANCE

4.1 Circuit Configuration

In the previous chapters we have seen as to how the i-v characteristics of a practical CCNR circuit can be made to approach that of an ideal pwL characteristics with controlled V_p, V_v, R_N etc by making the circuit more and more complex. However, for the experimental study of a relaxation oscillator, a very simple circuit configuration was used to determine the performance (temperature stability of the period of oscillation) that can be achieved.

The circuit diagram is shown in Figure 4.1. Q_1 forms the input transistor. Q_2, Q_3, Q_4 and Q_5 (CA 3086) form a current mirror of nominal gain 3. In order to compensate for the voltage drop of the emitter-base junction of the transistor Q_1, Q_6, Q_7 and Q_8 are used in the configuration shown in the Figure (See Appendix : CA 3084 has this structure available on the chip which is used to advantage). Thus the resistance of 40K appears as -120K (nominal) at the input terminals. V_p and V_v are defined using the resistor-divider chain.

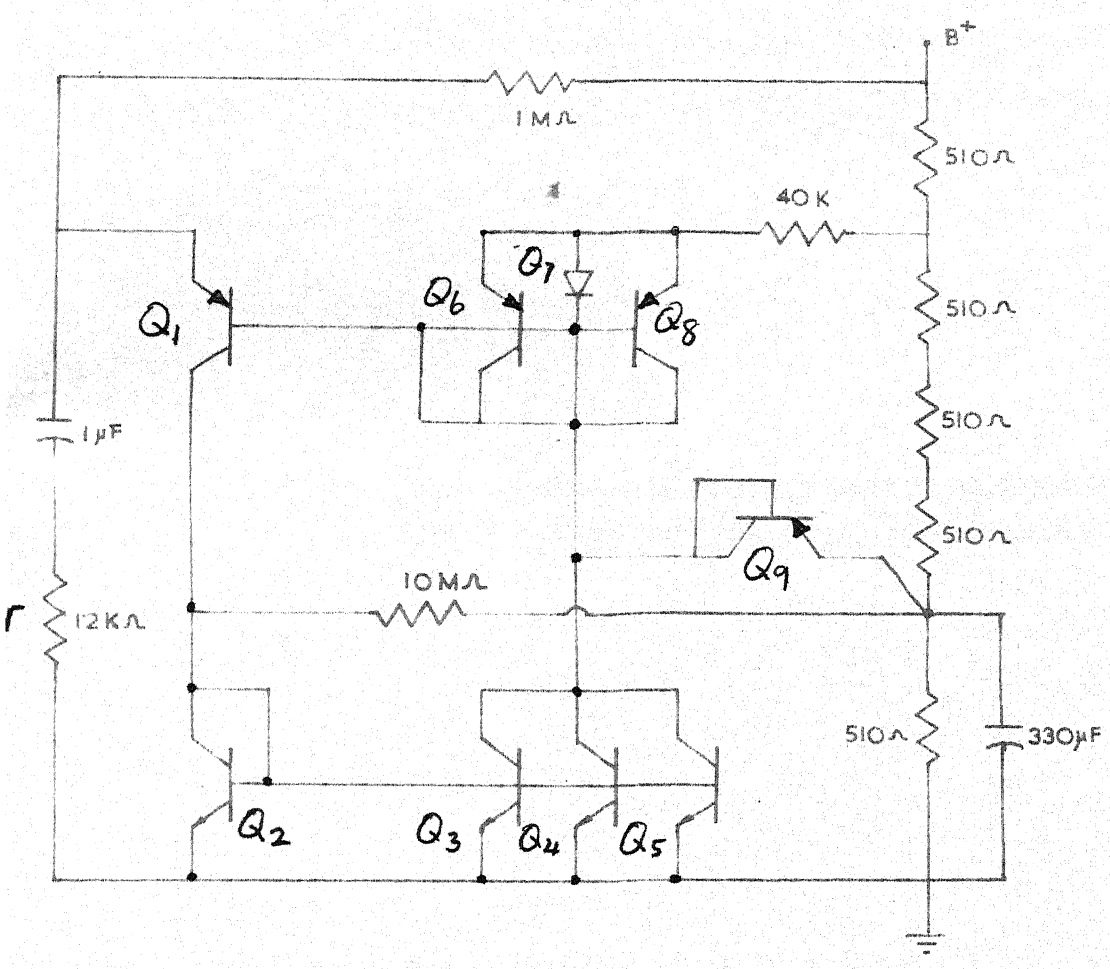

FIG. (5-1d)

RELAXATION OSCILLATOR
USING SIMPLE CCNR CIRCUIT

The transistor Q_9 is used to clamp the valley voltage approximately. It may be mentioned that this is an alternative by which the complementary NIC can be avoided especially when $R_p \to 0$ is desired (positive R_p can never be achieved this way). The temperature compensation, however, is not exact because the current following through Q_1 and Q_9 will never be exactly equal. But the max discharge current of the capacitor (limited by V) can be large (depending upon the choice of V), and thus the difference between the currents through the b-b junctions of Q_1 and Q_9 are different only by an amount equal to I_v which is kept in the order of 10 to 100μa.

The 10MΩ resistor connected as shown bleeds a small quescent current through the mirror as well as Q_6,Q_7 and Q_8 which is to prevent the overshoot around the peak voltage (as in the earlier circuits).

The use of a nominal gain of three in the mirror enables us to use a lower resistance to define R_N which reduces the power supply pick up as well as the voltage drop across the resistors due to reverse saturation currents as well as the current due to the 10MΩ resistor. A higher gain could be used with advantage but due to the restriction of the number of devices available on the CA 3084 chips this could not be employed.

4.2 Period of Oscillation

It can be seen from Figure (4.1b) that the region CD is almost vertical due to the clamping provided by the transistor Q_9. Neglecting the switching time, the period of oscillation is primarily governed by the time taken for the capacitor to

charge from V_v to V_p assuming that γ is negligibly small (10Ω). If r is the order of kilohms, the switching trajectory will be as shown by the dotted lines in Figure 4.1b. Under these conditions, the period of oscillation will be reduced since the voltage across the capacitor has to change only from V_D, to V_B.

If the resistance r is negligibly small, the period of oscillation for the scaling shown in Figure 4.1(a) will be $\tau \ln_e \frac{3}{4}$. The period is measured by the arrangement shown in Figure 4.2 where the sharp negative pulse across r during the discharge of the capacitor, is fed to the counter. It is experimentally observed that power line pick up, even if it is of the order of a millivolt will produce fluctuations in counts because its influence of V_p is obvious. The high level impedance at the base of the transistor Q_1 before it conducts can be very hig Thus extreme care has to be used in shielding the circuit using a metallic container.

4.3 Influence of I_{CO} of Q_1 on the Period of Oscillation

As was pointed out earlier, while the capacitor is charging, the emitter-base junction of the transistor Q_1 is reverse-biased. Its collector-base junction is reverse biased as well. The base is operated from a high impedance voltage source. Under these conditions, the current flowing into the emitter can be computed using Ebers-Moll relations and it will be in the order of I_{CO}. Typical value of I_{CO} measured is in the range of 0.1 na. Considering that the average charging

current is in the order of tens of micro-ampres, the influence of this is expected to be less than 1 part in 10^5. Although a first order compensation of this can be achieved, this was not attempted.

It was experimentally found that the short-term stability of the circuit was controlled by random fluctuations around the peak and valley voltages. Since the voltage difference between the peak and valley voltages is 6V (for a supply voltage of 10V), random drift around the peak and valley voltages of the order 6μV will produce fluctuations in the period by an amount equal to 1 part in 10^6 which is easily measured. The measured short-term stability (count to count) was in the order of one part in 10^5. The stability of the peak and valley points have to be determined separately by suitable experiments. However, this has not been done. It is envisaged that the randomness around the peak would be dominating factor in the short-term stability. Since the circuit is in a high impedence state around V_p whereas around V_v, the devices carry a fair amount of current.

4.4 Variation of the Period of Oscillation with Temperature

The variation of the period with temperature was studied by cooling the integrated transistor arrays alone to ice temperature. The results are as given below:

Period measured at room temperature 25°C 1352.11 msecs

Period measured at room temperature 1°C 1354.91

Thus the variation was 2.8 msecs in 1352 msecs which is approximately 86 ppm/°C. Since the saturation currents increase with temperature, the tendency for the peak voltage will be

to decrease with increase in temperature. Further the reverse saturation current of the emitter-base junction of Q_1 adds to the charging current. Thus, these effects add and make the period of ~~xx~~ oscillation decrease with temperature. The V_{BE} effects cancell because of the compensation scheme employed. Thus the experimental observation is consistent with the expected behaviour.

4.4 Variation of the Period of Oscillation with Supply Voltage

The variation of the period as a function of the supply voltage was determined experimentally. ~~Table~~ Fig 4.1 shows the results. The small variation really confirms that the peak and valley voltages vary linearly with the supply voltage. The small variation, however, is due to the non-linear effects such as the voltage dependence of the transistor parameters. This has not been computed using theoretical models. The variation in the period due to supply voltage change is estimated to be 75 ppm/volt (min)

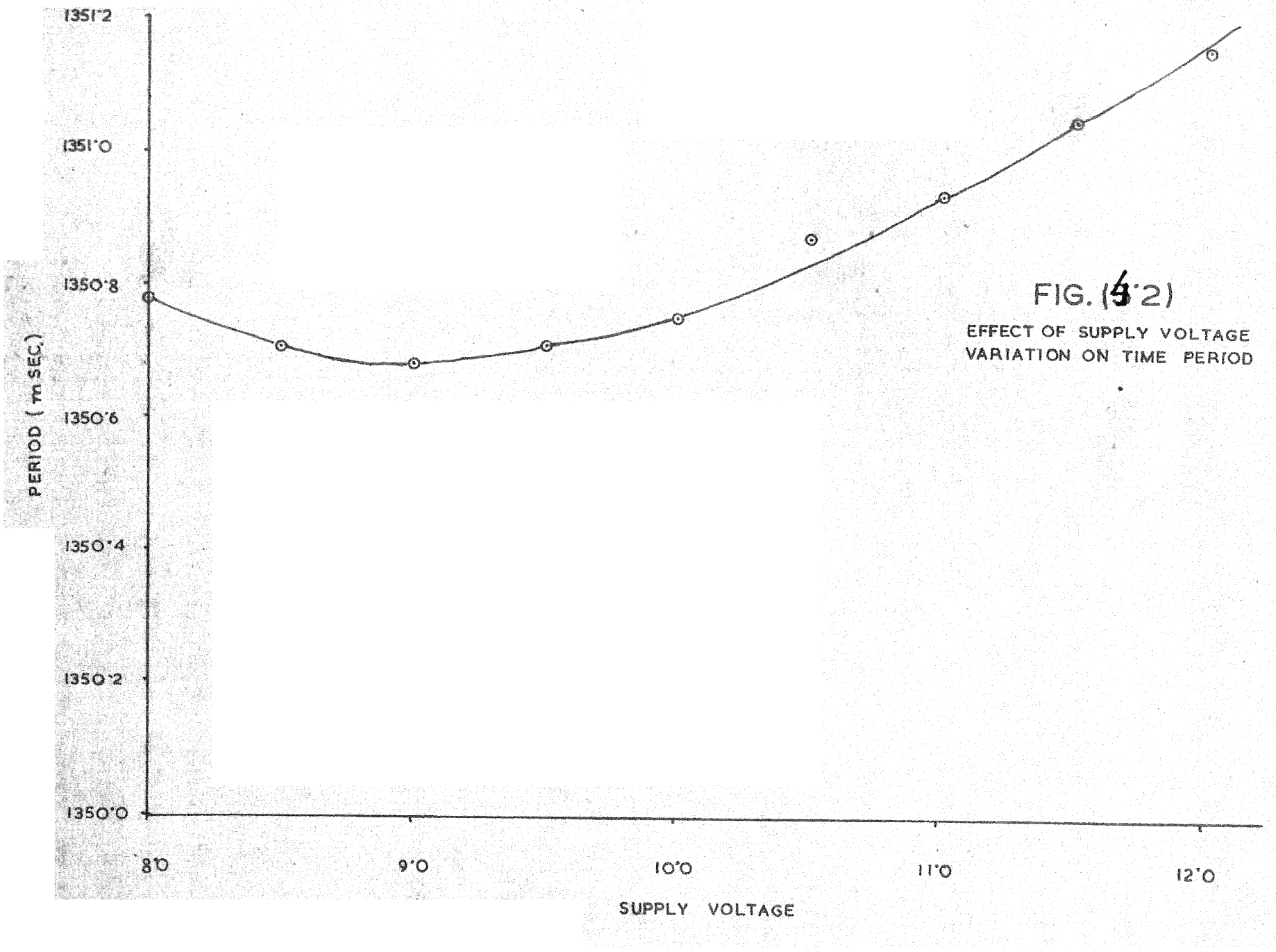

FIG. (4·2)

EFFECT OF SUPPLY VOLTAGE VARIATION ON TIME PERIOD

CHAPTER 5

CONCLUSION

The design of oscillators based on piece-wise linear CCNR, results in simple circuit configurations. Except for the timing elements, the circuit can be fabricated in integrated circuit form where the technology is used to advantage in obtaining the temperature compensated performance. While the present ivestigations show that the circuit is not good enough for watches, the circuit bridges a wide gap between the high precision crystal oscillators and ordinary multivibrators for many industrial timing applications. The quiscences can be made minimal which makes the circuit attractive for battery operated applications. No attempt has been made to match the temperature coefficients of the timing elements R and C which have to be done in order to investigate further improvement of the instability arising from the semi-conductor devices. As is clear, the compensation philosophy is based on matching of the transistors in the circuit. There are several more complex circuits which have to be investigated which would need computer-aided analysis. With the advent of ion-implanatation techniques, the degree of matching reported are incredibly low (a few microvolts in V_{BE} at quescent current levels as high as 1 ma). The lateral pnp transistors are well behaved at the low current levels they are employed.

The circuit configurations were restricted by the transistor arrays that were available. Thus the present study was restricted to simple structures and by and large the investigations were experimental and analysis very often qualitative.

REFERENCES

1. Silicon Gate CMOS Frequency Divider for Electronic Wrist-Watch
Eric Vittoz et al
IEEE Journal of Solid State Circuits, April 1972 (pp. 100-104).

2. Bipolar Micro-power Circuits for Crystal Controlled Time-Pieces
Heniz W. Resegg and Werner Thomson
IEEE Journal of Solid Skate Circuits, April 1972 (pp. 105-111).

3. Simple Negative Impedence Convertor
T.R. Viswanathan
Electronic Letters, August D 71 (pp. 501-502).

4. A Monolithic Junction FET - a npn Operational Amplifier
G.R. Wilson
IEEE Journal of Solid State Circuits, December 1968 (pp. 341-347).

5. Wave Generation and Shapping
Leonard Strauss
McGraw-Hill Book Co., 1970, pp. 509-510.

APPENDIX A

GENERAL-PURPOSE HIGH-CURRENT N-P-N TRANSISTOR ARRAY

CA3083

Features

High I_C: 100mA max.

Low V_{CEsat}(at 50 mA): 0.7V max.

Matched pair (Q1 and Q2) -

V_{IO}(V_{BE}matched): $\pm$ 5mV max.

V_{IO} (at 1mA): 2.5μA max.

5 independent transistors plus separate substrate connection.

Figure A1: Functional diagram of the CA3083

Maximum Ratings, Absolute-Maximum Values at T_A = 25°C

Power Dissipation:

Any one transistor		500	mW
Total package		750	mW
Above 25°C	Derate linearly	6.67	mW/°C

Ambient Temperature Range:

Operating	-40 to +85	°C
Storage	-55 to +150	°C

The following ratings apply for each transistor in the device:

Collector-to-Emitter Voltage (V_{CEO})	15	V
Collector-to-Base Voltage (V_{CBO})	20	V
Collector-to-Subtrate Voltage (V_{CIO})*	20	V
Emitter-to-Base Voltage (V_{EBO})	5	V
Collector Current (I_C)	100	mA
Base Current (I_B)	20	mA

*The collector of each transistor of the CA 3083 is isolated from the subtrate by an integral diode. The subtrate must be connected to a voltage which is more negative than any collector voltage in order to maintain isolation between transistors and provide normal transistor action. To avoid undesired coupling between transistors, the subtrate terminal (5) should be maintained at either DC or signal (AC) ground. A suitable bypass capacitor can be used to establish a signal ground.

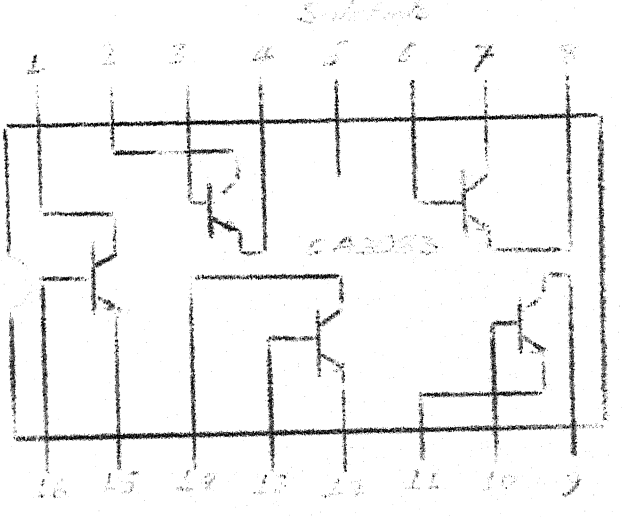

Fig. A.1 - Functional diagram of the CA3083

ELECTRICAL CHARACTERISTICS at T_A = 25°C
For Equipment Design

Characteristics	Symbol	TEST CONDITIONS	Typ. Char. Curve Fig. No.	LIMITS Min.	Typ.	Max.	Units
For Each Transistor							
Collector-to-Base Breakdown Voltage	$V_{(BR)CBO}$	I_C=100μA, I_E=0	-	20	60	-	V
Collector-to-Emitter Breakdown Voltage	$V_{(BR)CEO}$	I_C=1mA, I_B=0	-	15	24	-	V
Collector-to-Subtrate Breakdown Voltage	$V_{(BR)CIO}$	I_{CI}=100μA, I_B=0 I_E = 0	-	20	60	-	V
Emitter-to-Base Breakdown Voltage	$V_{(BR)EBO}$	I_E = 500μA, I_C=0	-	5	6.9	-	V
Collector-Cutoff-Current	I_{CEO}	V_{CE}=10V, I_B=0	-	-	-	10	μA
Collector-Cutoff-current	I_{CBO}	V_{CB}=10V, I_E=0	-	-	-	1	μA
DC Forward-Current Transfer Ratio	h_{FE}	V_{CE}=3V, I_C=10mA I_C=50mA	2	40 40	76 75	- -	
Base-to-Emitter Voltage	V_{BE}	V_{CE}=3V, I_C=10mA	3	0.65	0.74	0.85	V
Collector-to-Emitter Saturation Voltage	V_{CEsat}	I_C=50mA, I_B=5mA	4	-	0.40	0.70	V

Characteristics	Symbol	TEST CONDITIONS	Typ. Char. Curve Fig. No.	Min.	Typ.	Max.	Units
For Transistors Q1 and Q2 (As a Differential Amplifier):							
Absolute Input Offset Voltage	V_{IO}	V_{CE}=3V, I_C=1mA	7	-	1.2	5	mV
Absolute Input Offset Current	I_{IO}	V_{CE}=3V, I_C=1mA	8	-	0.7	2.5	μA

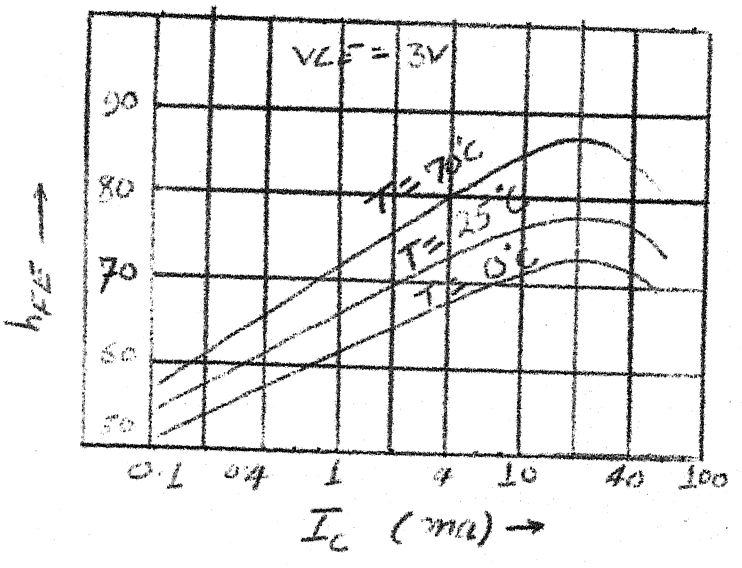

Fig A2: h_{FE} vs. I_C

APPENDIX B

GENERAL-PURPOSE P-N-P TRANSISTOR ARRAY

CA3084

Features

Matched transistor pair (Q1 and Q2)

V_{IO}(V_{BE} matched): ±6mV max.

I_{IO}(at 100 A) : ± 0.6μA

Wide operating current range

Low noise figure 3.2dB typ. at 1kHz

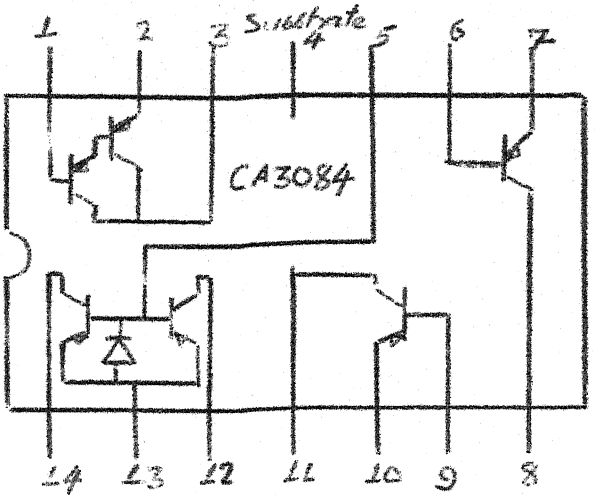

Figure B1: Functional Diagram of the CA3084.

ELECTRICAL CHARACTERISTICS at T_A= 25°C

CHARACTERS	SYMBOL	TEST CONDITIONS	Typ. Characteristics Curve Fig.No.	LIMITS Min.	Typ.	Max.	Units
For Each Transistor:							
Collector-Cutt-off current	I_{CBO}	V_{CB}=-10V,I_E=0	2	-	-0.055	-100	nA

CHARACTERS	SYMBOL	TEST CONDITIONS	Typ. Characteristics Curve Fig.No.	LIMITS Min.	Typ.	Max.	Units
Collector-Cuttoff Current	I_{CBO}	V_{CE}=-10V, I_E=0	2	-	-0.12	-100	nA
Collector-to-Emitter Breakdown Voltage	$V_{(BR)CEO}$	I_{CE}=-100μA, I_B=0	-	-40	-70	-	V
Collector-to-Base Breakdown Voltage	$V_{(BR)CBO}$	I_{CB}=-100μA, I_E=0	-	-40	-80	-	V
Emitter-to-Base Breakdown Voltage	$V_{(BR)EBO}$	I_{EB}=100μA, I_C=0	-	-40	-100	-	V
Emitter-to-Substrate Breakdown Voltage	$V_{(BR)EIO}$	I_{EI} = 100μA	-	-40	-100	-	V
Collector-to-Emitter Saturation Voltage	V_{CEsat}	I_E=1mA, I_B=100μA	4	-	-0.125	-0.25	V
Base-to-Emitter Voltage	V_{BE}		5	-0.50	-0.59	-0.68	V
DC Forward Current Transfer Ratio	h_{FE}	I_E=100μA, V_{CE}=-10V	7	15	40	-	
For Transistor Q1 and Q2 (As a Differential Amplifier)							
Magnitude of Input Offset Voltage	$\lvert V_{IO} \rvert$	I_E=100μA, V_{CE}=-10V	8	-	0.422	6	mV
Input Offset Current	I_{IO}		-	-0.6	0	0.6	μA

CHARACTERISTICS	SYMBOL	TEST CONDITIONS	Typ. Characteristics Curve Fig.No.	LIMITS Min.	Typ.	Max.	Units
For Transistors Q3 and Q4 (Current-Mirror Configuration)							
Collector Current	I_C	V_{CE}=-10V, V_{CIO}=-10V	10	0.85	1.00	1.15	µA
Magnitude of Collector Current Ratio	$\lvert I_C(Q3)/I_C(Q4)\rvert$	Term. 13 = Gnd. I_5 = -100µA	11	0.90	1.00	1.10	
For Transistors Q5 and Q6 (Darlington Configuration)							
Collector-Cutoff Current	I_{CEO}	V_{CE}=-10V, I_B=0	-	-	-	-1.0	µA
Base-to-Emitter Voltage	I_{CEO}		13	0.92	1.07	1.20	V
DC Forward Current Transfer Ratio	h_{FE}	I_E=100µA, V_{CE}=-10V	15	100	1230	-	

ELECTRICAL CHARACTERISTICS at T_A = 25°C
Typical Values Intended Only for Design Guidance

Magnitude of Temperature Coefficient						
V_{BE} (for each transistor)	$\lvert\Delta V_{BE}/\Delta T\rvert$	I_E=100 A, V_{CE}=-10V	6		-1.78	mV/°
V_{IO} (as a differential amplifier)	$\lvert\Delta V_{IO}/\Delta T\rvert$		9		0.54	µV/°
V_{BE} (Darlington configuration)	$\lvert\Delta V_{BE}/\Delta T\rvert$		14		-3.7	mV/°
For Each Transistor:						
Input Resistance	R_1	f=1kHz, V_{CE}=-10V	19	-	9	kΩ
Output Resistance	R_O		20	-	600	- kΩ
Forward Transconductors	g_m	I_C=-100µA	22	-	3	- mmho

CHARACTERISTICS	SYMBOL	TEST CONDITIONS	Typ. Characteristics Curve Fig.No.	LIMITS Min.	Typ.	Max.	Units
Collector-to-Base-Capacitance	C_{CBO}	$I_{CB} = 0$	23	-	3.3	-	pF
Collector-to-Emitter Capacitance	C_{CEO}	$I_{CE} = 0$	23	-	2.5	-	pF
Base-to-Substrate Capacitance	C_{BIO}	$I_{CIO} = 0$	23	-	4.5	-	pF

MAXIMUM RATINGS, Absolute-Maximum Values at T_A=25°C

Dissipation:

Any one transistor	200	mW
Total package	750	mW
Above T_A=55°C derate linearly	6.67	mW/°C

Ambient Temperature Range:

Operating	-40 to +85	°C
Storage	-55 to +150	°C

The following ratings apply for each transistor in the device:

Collector-to-Emitter Voltage (V_{CEO})	-40	V
Collector-to-Base Voltage (V_{CBO})	-40	V
Base-to-Substrate Voltage (V_{BIO})*	-40	V
Emitter-to-Base Voltage (V_{EBO})	-40	V
Collector Current (I_C)	-10	mA

*The base of each transistor of the CA3084 is isolated from the substrate by an integral diode. The substrate must be connected to a voltage which is more negative than any base voltage in order to maintain isolation between transistors and provide normal transistor action. To avoid undesired coupling between transistors, the substrate terminal (4) should be maintained at either DC or signal (AC) ground. A suitable bypass capacitor can be used to estalish a signal ground.

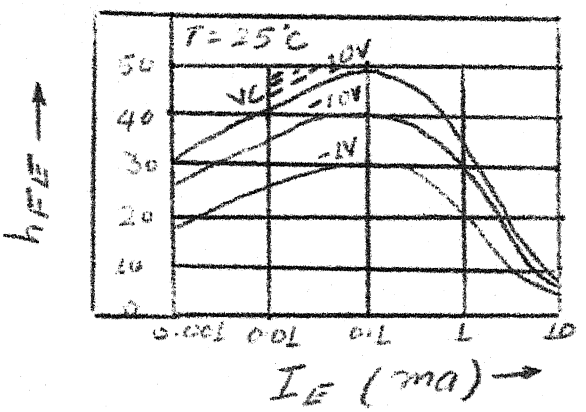

Fig. B2: h_{FE} Vs. I_E

APPENDIX C

GENERAL-PURPOSE N-P-N TRANSISTOR ARRAY

CA3086

Three isolated Transistors and One Differentially Connected Transistor Pair

For Low-Power Applications from DC to 120MHz

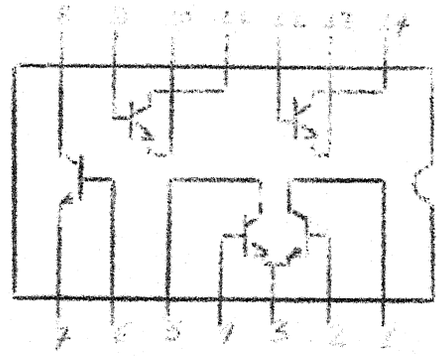

Figure C1: Functional Diagram of the CA3086.

MAXIMUM RATINGS, Absolute Values (Maximum) at T_A = 25°C

Dissipation:

Any one transistor		300	mW
Total package		750	mW
Above T_A=25°C	derate linearly	6.67	mW/°C

Ambient Temperature Range:

Operating	-40 to +85	°C
Storage	-55 to + 150	°C

The following ratings apply for each transistor in the device:

Collector-to-Emitter Voltage, V_{CEO}	15	V
Collector-to-Base Voltage, V_{CBO}	20	V
Collector-to-Substrate Voltage, V_{CIO}*	20	V
Emitter-to-Base Voltage, V_{EBO}	5	V
Collector Current, I_C	50	mA

*The collector of each transistor in the CA3086 is isolated from the substrate by an integral diode. The substrate (terminal 13) must be connected to the most negative point in the external circuit to maintain isolation between transistors and to provide for normal transistor action. To avoid undesirable coupling between transistors, the substrate (terminal 13) should be maintained at either DC or signal (AC) ground. A suitable bypass capacitor can be used to establish a signal ground.

ELECTRICAL CHARACTERISTICS at T_A = 25°C

CHARACTERISTICS	SYMBOLS	TEST CONDITIONS	Typ. Characteristics Curves Fig.No.	LIMITS Min.	Typ.	Max.	Units
Collector-to-Base Breakdown Voltage	$V_{(BR)CBO}$	I_C=10μA; I_E=0	-	20	60	-	V
Collector-to-Emitter Breakdown Voltage	$V_{(BR)CEO}$	I_C=1mA, I_B=0	-	15	24	-	V
Collector-to-Substrate Breakdown Voltage	$V_{(BR)CIO}$	I_C=10μA, I_{CI}=0	-	20	60	-	V
Emitter-to-Base Breakdown Voltage	$V_{(BR)EBO}$	I_E=10μA, I_C=0	-	5	7	-	V
Collector-cutoff Current	I_{CBO}	V_{CB}=10V, I_E=0	2	-	0.002	100	nA
Collector-Cutoff Current	I_{CEO}	V_{CE}=10V, I_B=0	3	-	See Curve	5	μA
DC Forward Current Transfer Ratio	h_{FE}	V_{CE}=3V, I_C=1mA	4	40	100	-	

ELECTRICAL CHARACTERISTICS at T_A=25°C
Typical Values Intended Only to Design Guidance

CHARACTERISTICS	SYMBOL	TEST CONDITIONS	Typ. Characteristics Curves Fig.No.	Typical Values	Units
DC Forward-Current Transfer Ratio	h_{FE}	V_{CE}=3V I_C=10mA	4	100	
		I_C=10μA	4	54	
Base-to-Emitter Voltage	V_{BE}	V_{CE}=3V I_E=1mA	5	0.715	V
		I_E=10mA	5	0.800	V
V_{BE} Temperature coefficient	$\Delta V_{BE}/\Delta T$	V_{CE}=3V, I_C=1mA	6	-1.9	mV/°C
Collector-to-Emitter Saturation Voltage	V_{CEsat}	I_B=1mA, I_C=10mA	-	0.23	V
Noise Figure (low frequency)	NF	f=1kHz, V_{CE}=3V, I_C=100μA, R_S=1kΩ	-	3.25	dB
Low-Frequency, Small-Signal Equivalent-Circuit Characteristics					
Forward Current Transfer Ratio	h_{fe}		7	100	-
Short-Circuit Input Impedance	h_{ie}	f=1kHz, V_{CE}=3V, I_C=1mA	7	3.5	kΩ
Open-Circuit Output Impedance	h_{oe}		7	15.6	μmho
Open-circuit Reverse-Voltage Transfer Ratio	h_{re}		7	$1.8X10^{-4}$	-
Admittance Characteristics:					
Forward Transfer Ratio	y_{fe}		8	31-j1.5	mmho

CHARACTERISTICS	SYMBOL	TEST CONDITIONS	Typ. Characteristics Curves Fig. No.	Typical Values	Units
Input Admittance	y_{ie}	f=1MHz, V_{CE}=3V, I_C=1mA	9	0.3+j0.04	mmhc
Output Admittance	y_{oe}		10	0.001+j0.03	mmhc
Reverse Transfer Admittance	y_{re}		11	See Curve	-
Gain-Bandwidth Product	f_T	V_{CE}=3V, I_C=3mA	12	550	MHz
Emitter-to-Base Capacitance	C_{EBO}	V_{EB}=3V, I_E=0	-	0.6	pF
Collector-to-Base Capacitance	C_{CBO}	=3V, I_C=0	-	0.58	pF
Collector-to-Substrate Capacitance	C_{CIO}	=3V, I_C=0	-	2.8	pF

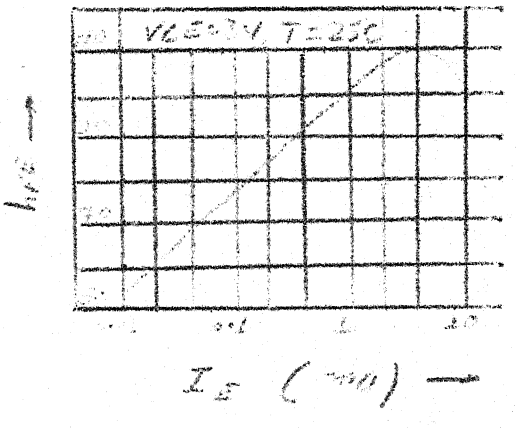

Fig C2: h_{FE} Vs. I_E